Chemistry–A European Journal

Supporting Information

Dithiolopyrrolones are Prochelators that are Activated by Glutathione

Francesca Albini, Stefan Bormann, Philipp Gerschel, Veza A. Ludwig, and Wilma Neumann*

This Supporting Information includes:

General Materials and Methods

Reagents. All commercially available reagents were sourced from Alfa Aesar, Sigma-Aldrich, Acros Organics, Carl Roth, TCI Europe, or VWR, and used without further purification. An MBRAUN SPS system was used to dry THF; anhydrous DMF was purchased from Sigma-Aldrich.

Chromatography. Analytical thin layer chromatography (TLC) was performed on pre-coated aluminum plates (silica gel 60 F254, Merck), which were analyzed employing UV light (254 nm) and an iodine chamber. Flash chromatography was performed with silica gel (0.06–0.2 mm, 60 M; Machery-Nagel). RP-HPLC was performed on a KNAUER HPLC system with a solvent system, A: 0.1% TFA in HPLC-grade H_2O, B: 0.1% TFA in HPLC-grade CH_3CN. Absorbance was detected with a multi-wavelength detector at the specified wavelengths (220 nm; 280 nm (specific for DTT_{ox} and Holo), or 330 nm and 380 nm (specific for Holo). Analytical RP-HPLC was performed using a Nucleodur column (100-3 C18 ec, 3 µm particle size, 4 mm ID x 125 mm, Machery-Nagel), operated at a flow rate of 1 mL/min was applied, and gradient-1: 10% B for 1 min, followed by 10%→66% B over 14 min, or gradient-2: 10% B for 1 min, 10→90% B over 20 min (used for purity analysis).

NMR. ^{1}H and ^{13}C NMR spectra were recorded on a Bruker DRX 400 and a Bruker AVIII 400; ^{19}F NMR were recorded on a Bruker DPX 250 NMR spectrometer. The chemical shifts are given in ppm relative to the residual solvent peak ($CDCl_3$, 7.26 ppm for ^{1}H; DMSO-d_6: 2.50 ppm for ^{1}H, 39.52 ppm for ^{13}C); for ^{19}F NMR, the spectra were referenced through the solvent lock (^{2}H) signal according to the IUPAC recommended secondary referencing method.[1] Multiplicities are reported using the following abbreviations: s, singlet; br s, broad singlet; t, triplet; q, quadruplet.

MS. HR-ESI-MS measurements were performed on a Vion IMS QToF (Waters) system in positive mode, with compounds dissolved in CH_3CN.

UV-vis spectroscopy. Optical absorption spectra were recorded on a Jasco V-670 spectrophotometer operated at ambient temperature in single-use UV-cuvettes (1 cm; BRAND).

Methods References

1. Harris RK; Becker ED; Cabral de Menezes SM; Goodfellow R; Granger P. NMR nomenclature. Nuclear spin properties and conventions for chemical shifts (IUPAC Recommendations 2001). *Pure Appl. Chem.* **2001**, *73*, 1795–1818.

Supporting Figures

1) Redox Mechanisms

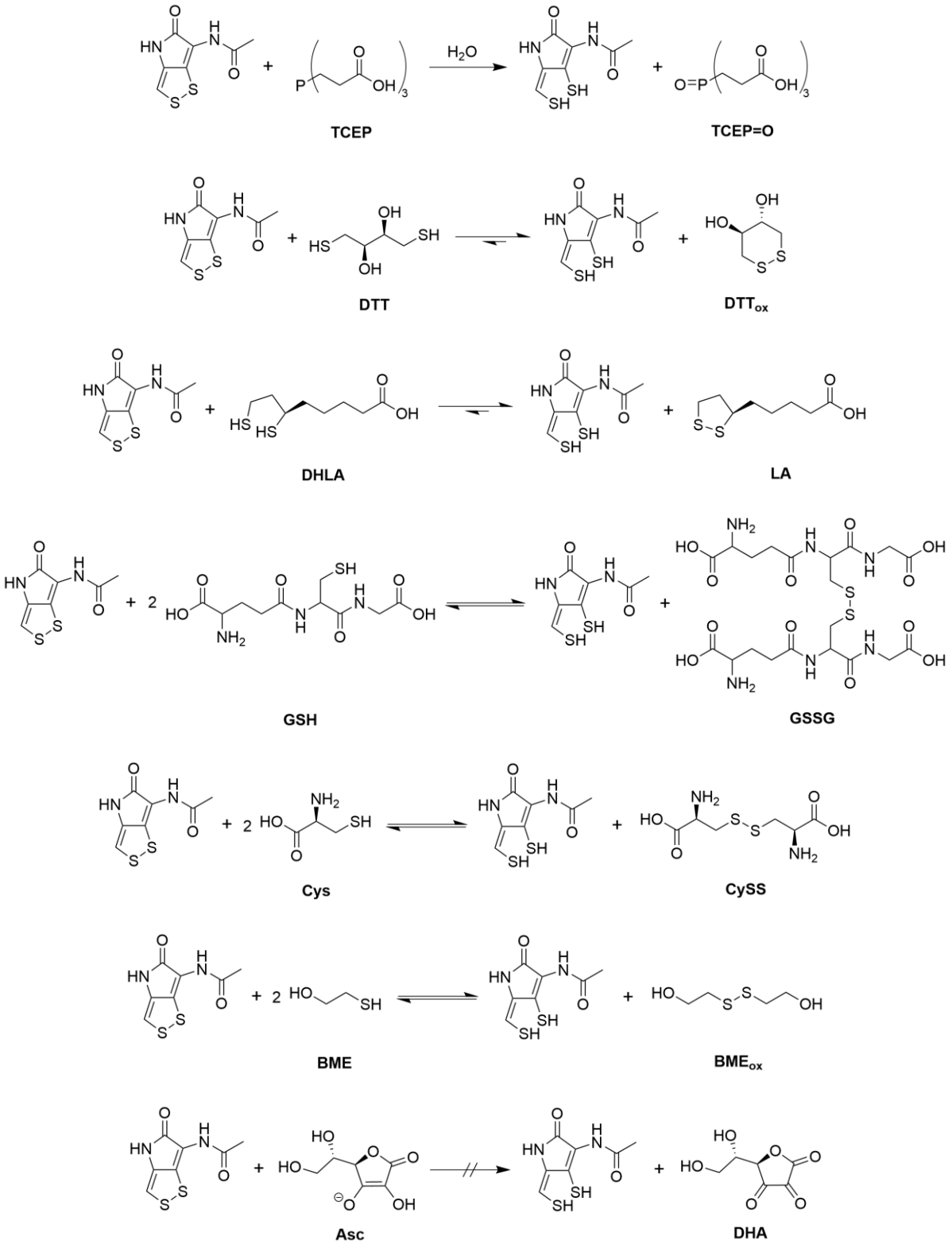

Scheme S1. Reactions of Holo with different reducing agents.

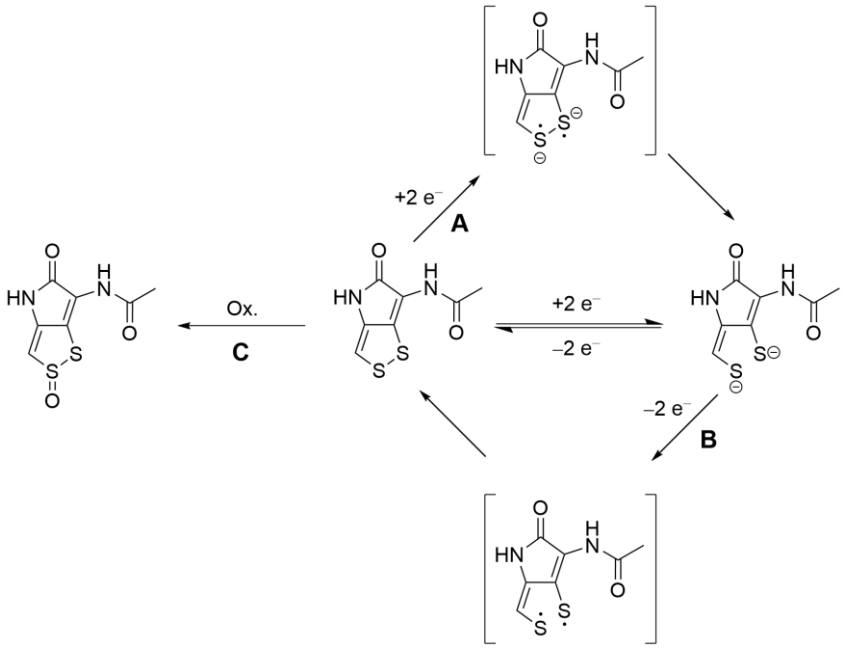

Scheme S2. Molecular pathways during CV of Holo. (A) Cathodic peak; (B) 1st anodic peak; (C) 2nd anodic peak.

2) UV-vis Assays

2.1) Titration with reducing agents

A **B**

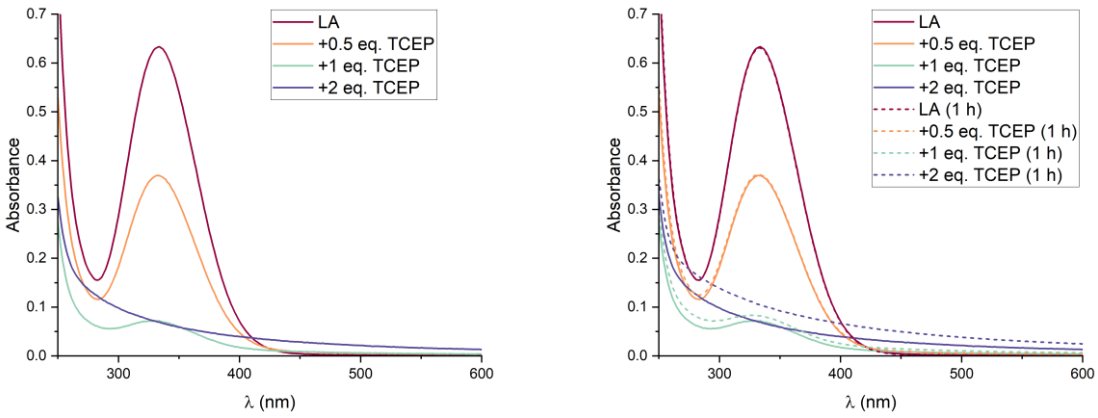

Fig. S1. Reduction of LA with TCEP. (A) Titration with TCEP. (B) Stability of the formed DHLA over 1 h in the presence of air. The titrations were performed with 5 mM LA in 75 mM Tris-HCl, pH 7.4.

A **B**

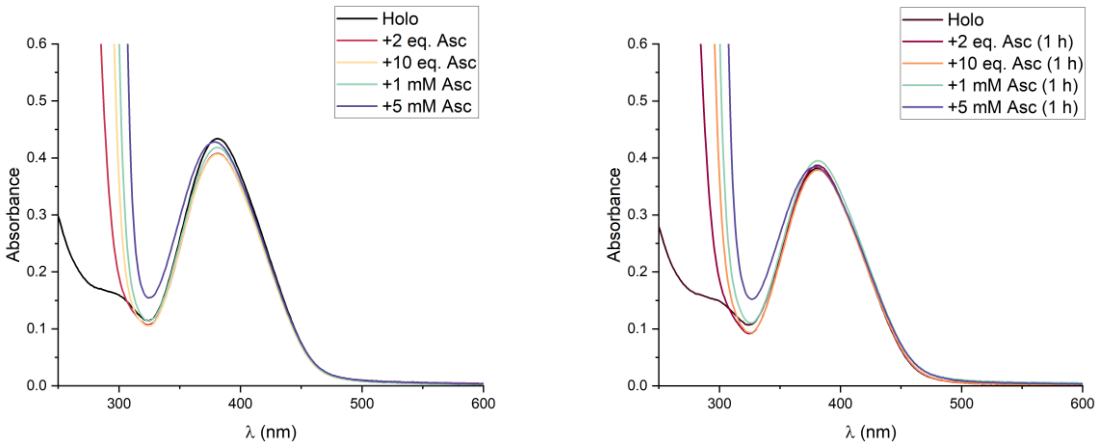

Fig. S2. Incubation of Holo with Asc. (A) Titration with Asc. (B) After incubation for 1 h. The titrations were performed with 50 µM Holo in 75 mM Tris-HCl, pH 7.4.

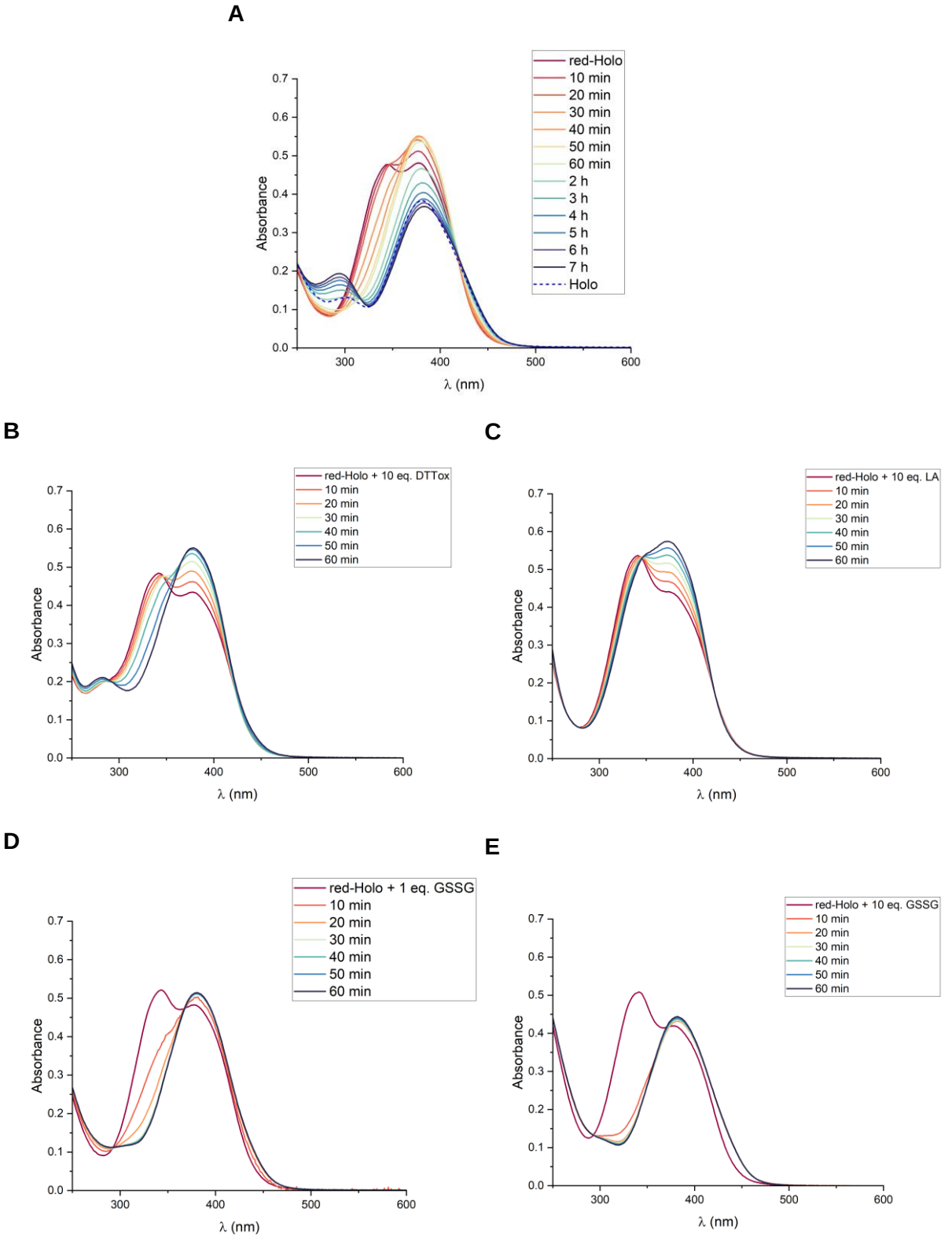

Fig. S3. Re-oxidation of *red*-Holo on air. (A) Re-oxidation of *red*-Holo. Re-oxidation of *red*-Holo in the presence of 10 eq. DTT_{ox} (B) (absorption at 280 nm originates from DTT_{ox}), 10 eq. LA (C) (the extinction of LA impacts the appearance of the spectrum), 1 eq. GSSG (D), 10 eq. GSSG (E). The incubations were performed with 50 µM *red*-Holo (reduced with 1 eq. TCEP) in 75 mM Tris-HCl, pH 7.4.

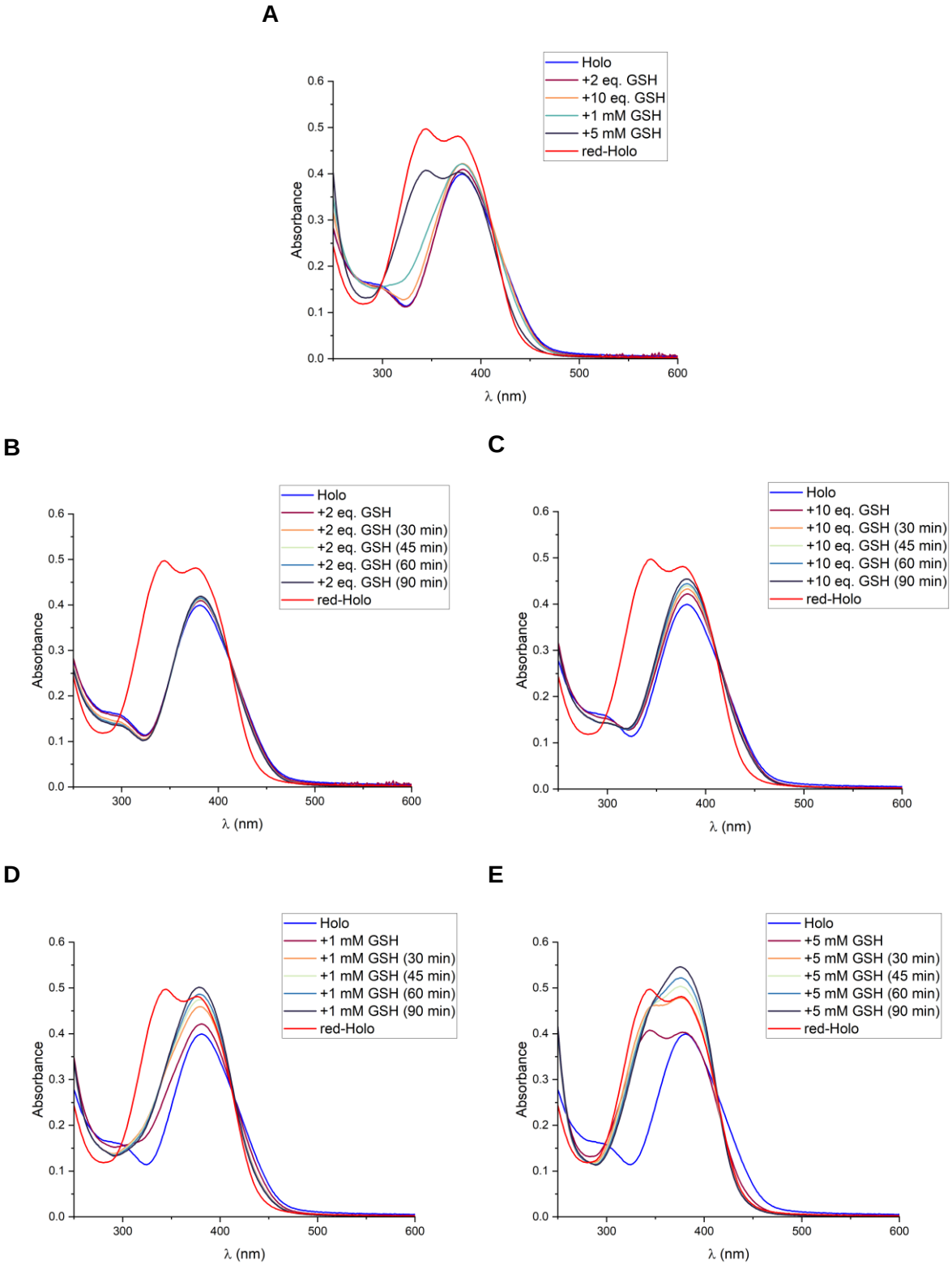

Fig. S4. Reduction of Holo with GSH. (A) Titration with GSH. Incubation with 2 eq. (B), 10 eq. (C), 1 mM (D), or 5 mM GSH (E). The titrations were performed with 50 µM Holo in 75 mM Tris-HCl, pH 7.4. Data of (A) is also shown in Fig. 3 in the main text, but included here to ease comparison.

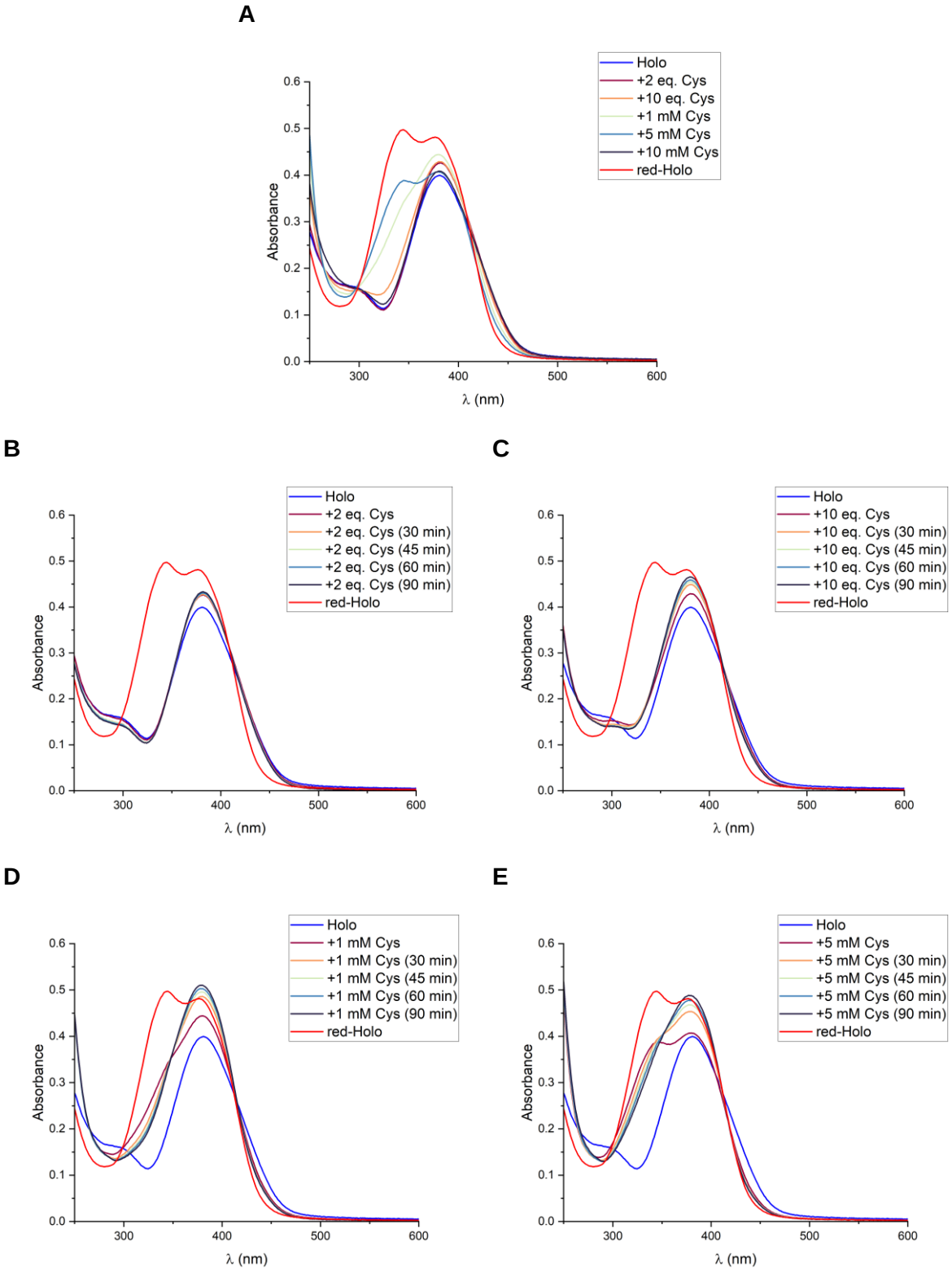

Fig. S5. Reduction of Holo with Cys. (A) Titration with Cys. Incubation with 2 eq. (B), 10 eq. (C), 1 mM (D), or 5 mM Cys (E). The titrations were performed with 50 µM Holo in 75 mM Tris-HCl, pH 7.4.

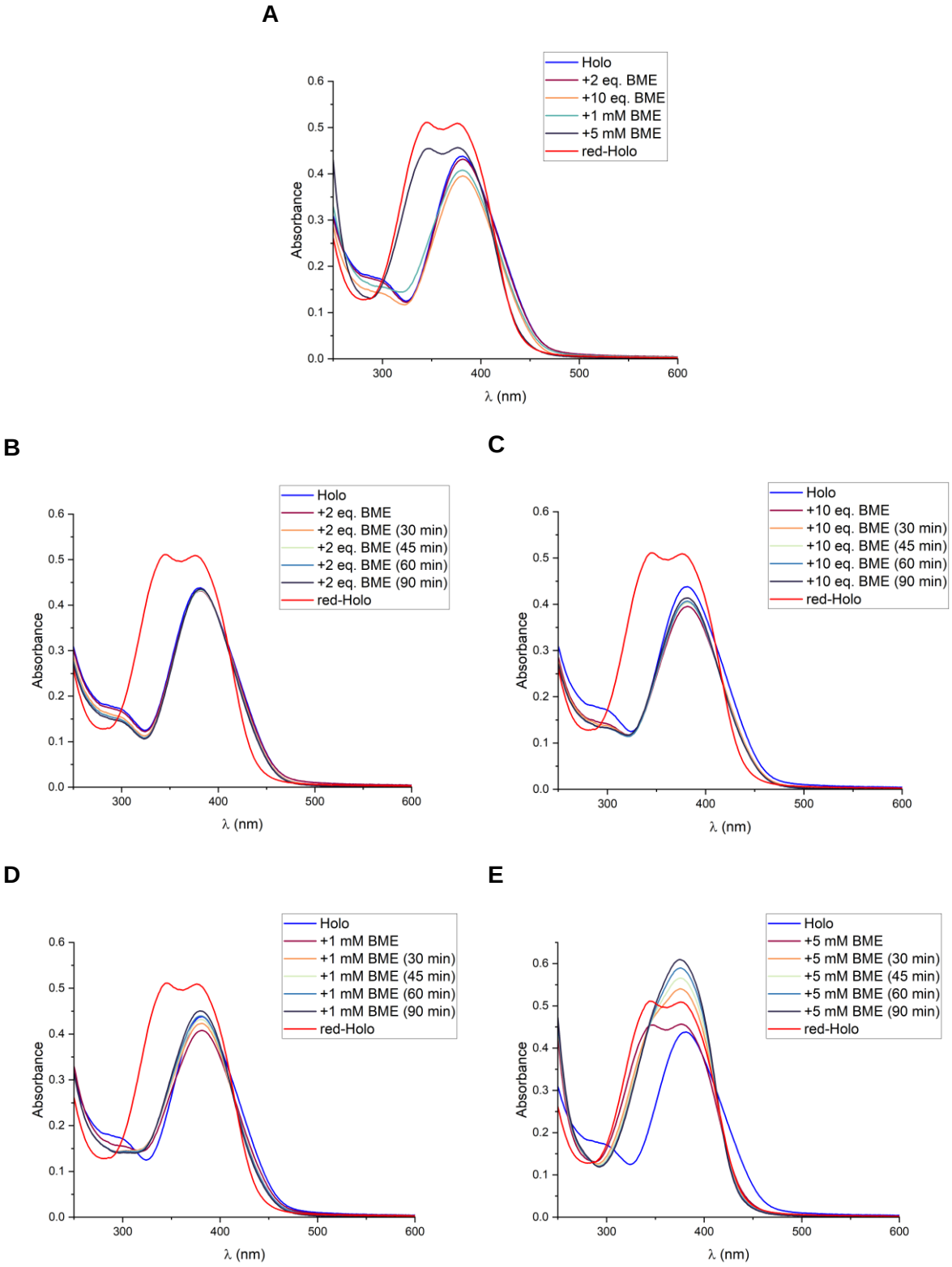

Fig. S6. Reduction of Holo with BME. (A) Titration with BME. Incubation with 2 eq. (B), 10 eq. (C), 1 mM (D), or 5 mM BME (E). The titrations were performed with 50 µM Holo in 75 mM Tris-HCl, pH 7.4.

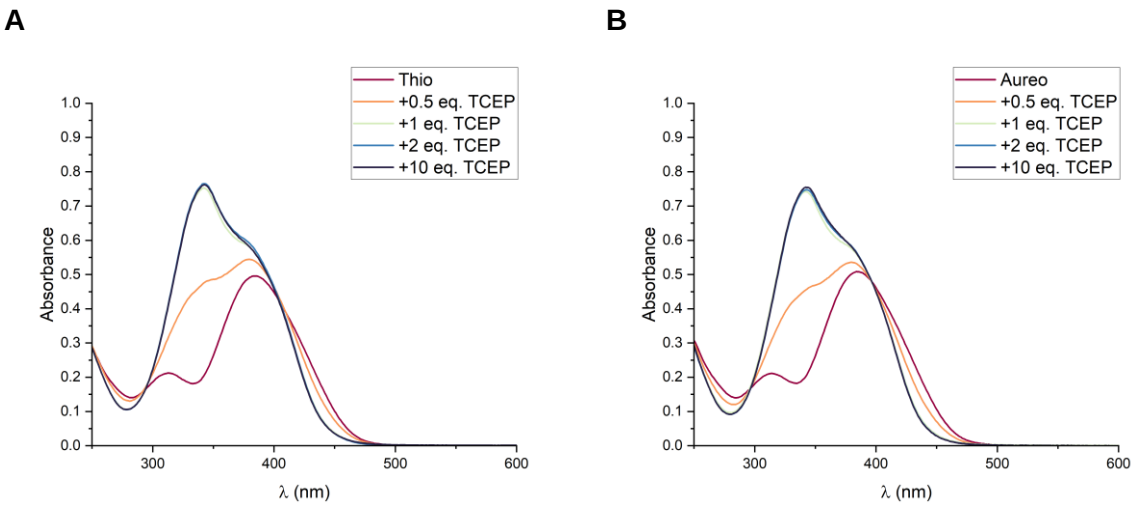

Fig. S7. Reduction of thiolutin and aureothricin with TCEP. (A) Titration of thiolutin. (B) Titration of aureothricin. The titrations were performed with 50 µM DTP in 75 mM Tris-HCl, pH 7.4.

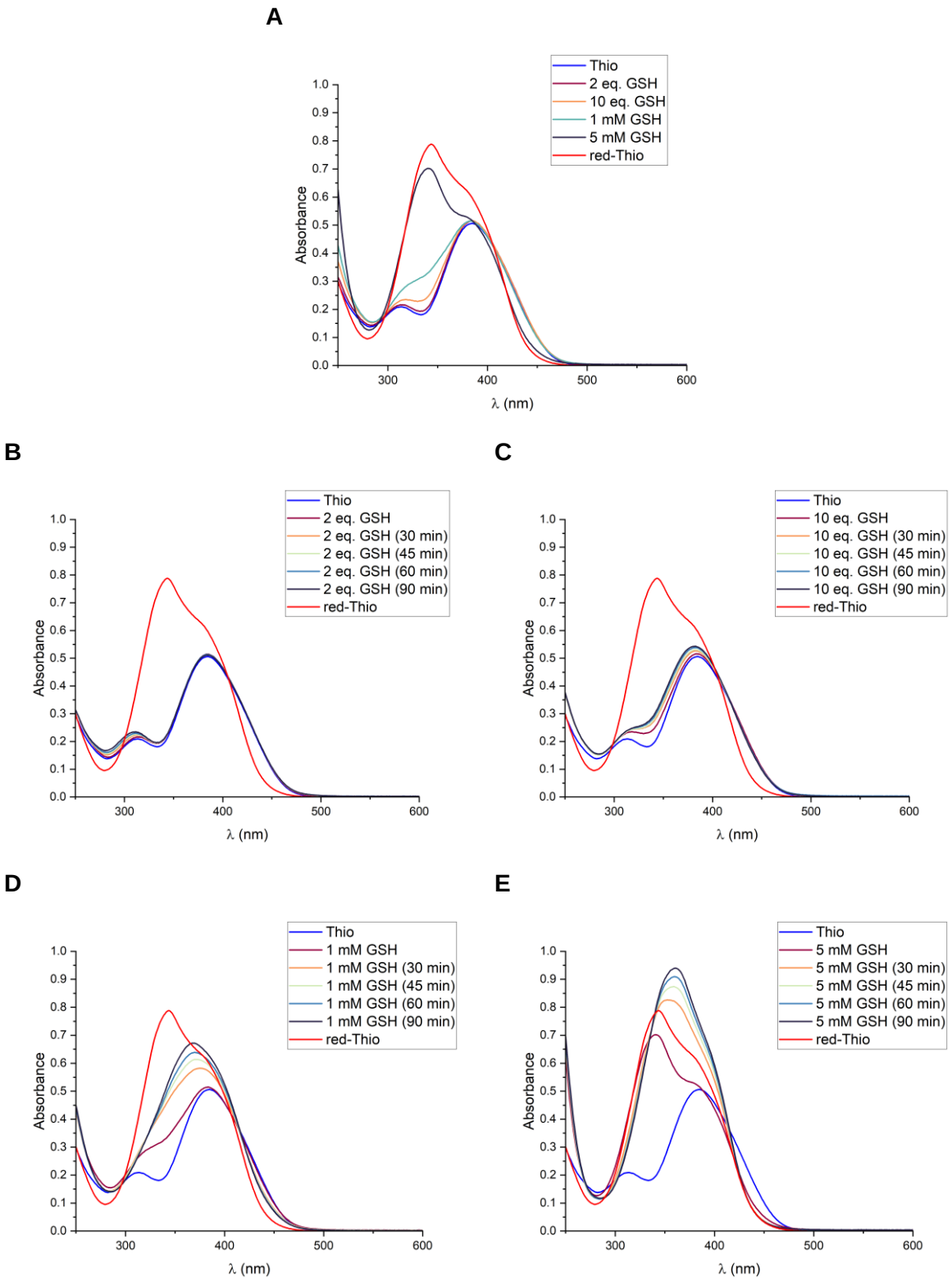

Fig. S8. Reduction of thiolutin with GSH. (A) Titration with GSH. Incubation with 2 eq. (B), 10 eq. (C), 1 mM (D), or 5 mM GSH (E). The titrations were performed with 50 µM thiolutin in 75 mM Tris-HCl, pH 7.4.

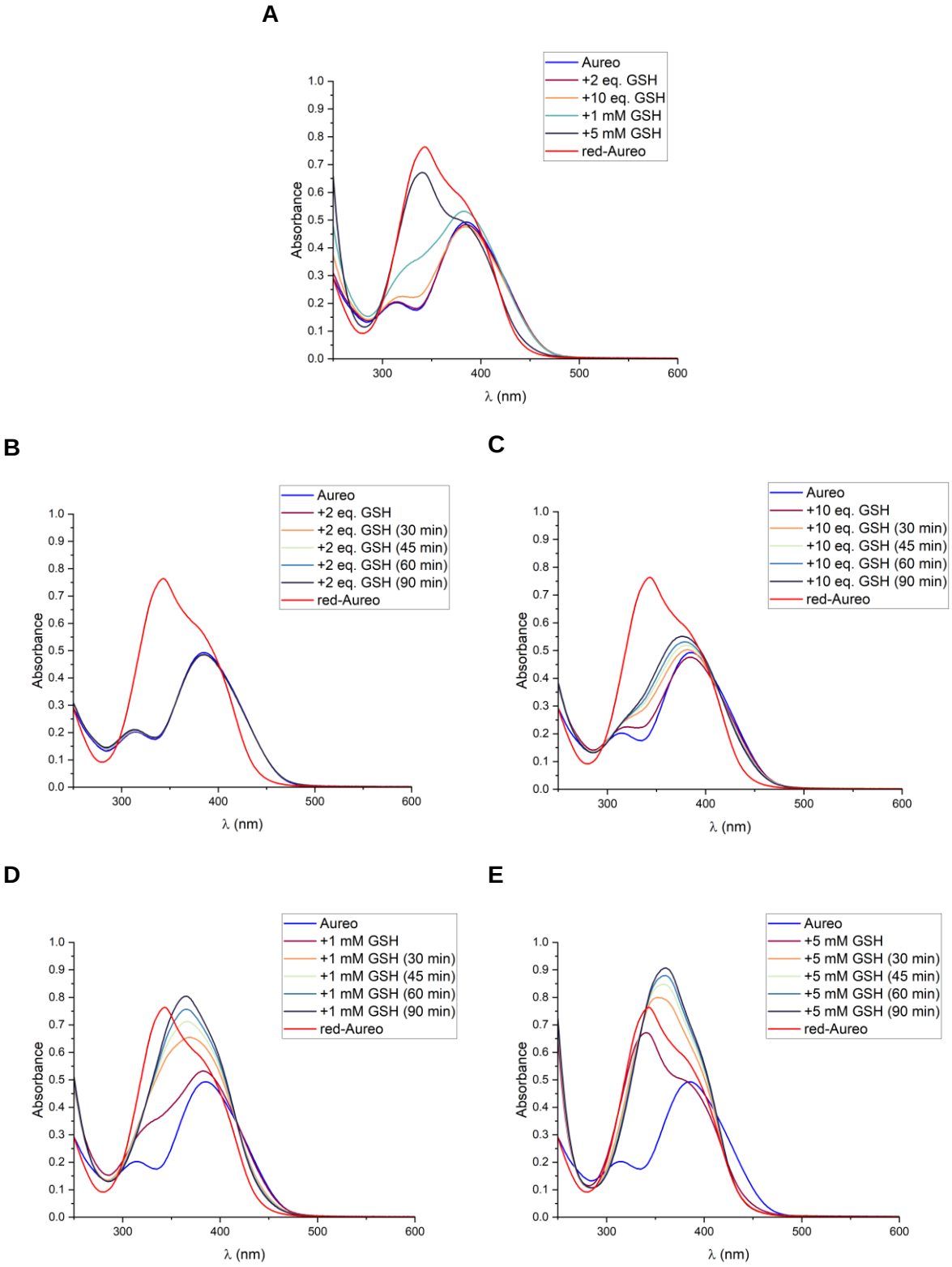

Fig. S9. Reduction of aureothricin with GSH. (A) Titration with GSH. Incubation with 2 eq. (B), 10 eq. (C), 1 mM (D), or 5 mM GSH (E). The titrations were performed with 50 µM aureothricin in 75 mM Tris-HCl, pH 7.4.

2.2) Zn(II) Coordination

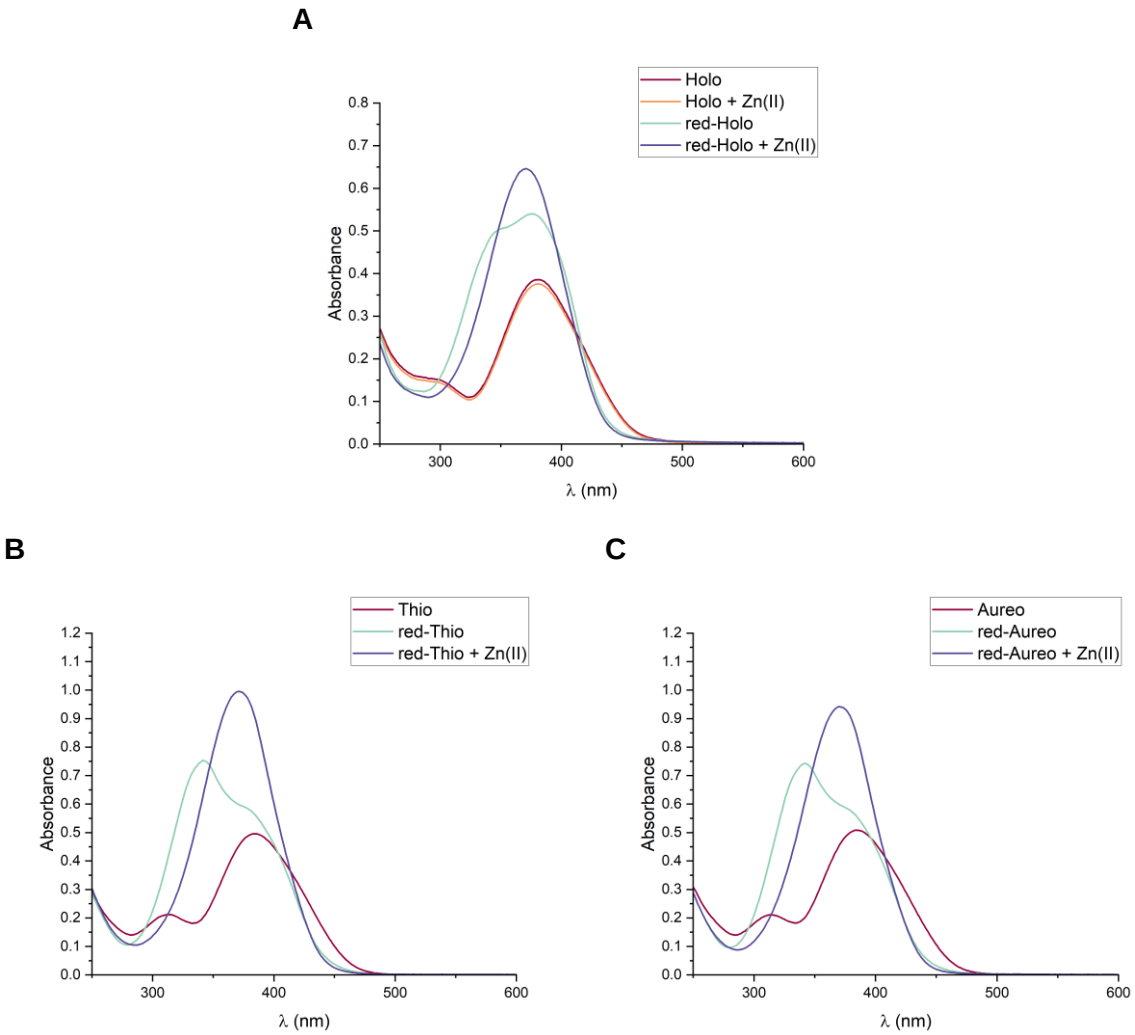

Fig. S10. Coordination of *red*-DTPs to Zn(II). (A) Reduction of Holo is required for metal coordination.Holo and *red*-Holo were incubated with Zn(II). (B) Coordination of *red*-thiolutin to Zn(II). (C) Coordination of *red*-aureothricin to Zn(II). The assays were performed with 50 µM DTP or *red*-DTP (reduced with 1 eq. TCEP) and addition of 0.5 eq. Zn(II) in 75 mM Tris-HCl, pH 7.4.

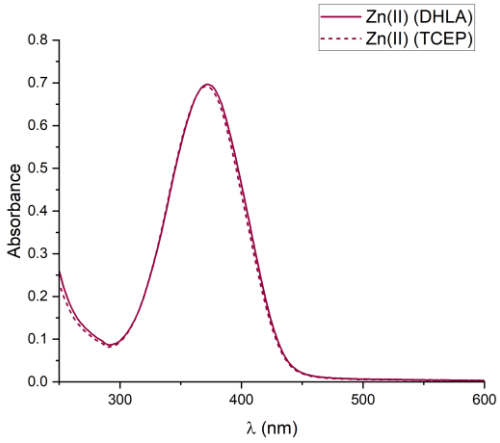

Fig. S11. Zn(II) coordination of Holo mediated by DHLA. Holo was reduced with DHLA and incubated with Zn(II). The assay was performed with 50 µM *red*-Holo (reduced with 1 eq. DHLA) and addition of 0.5 eq. Zn(II) in 75 mM Tris-HCl, pH 7.4. The spectrum of the complex of Holo reduced with TCEP is included for comparison.

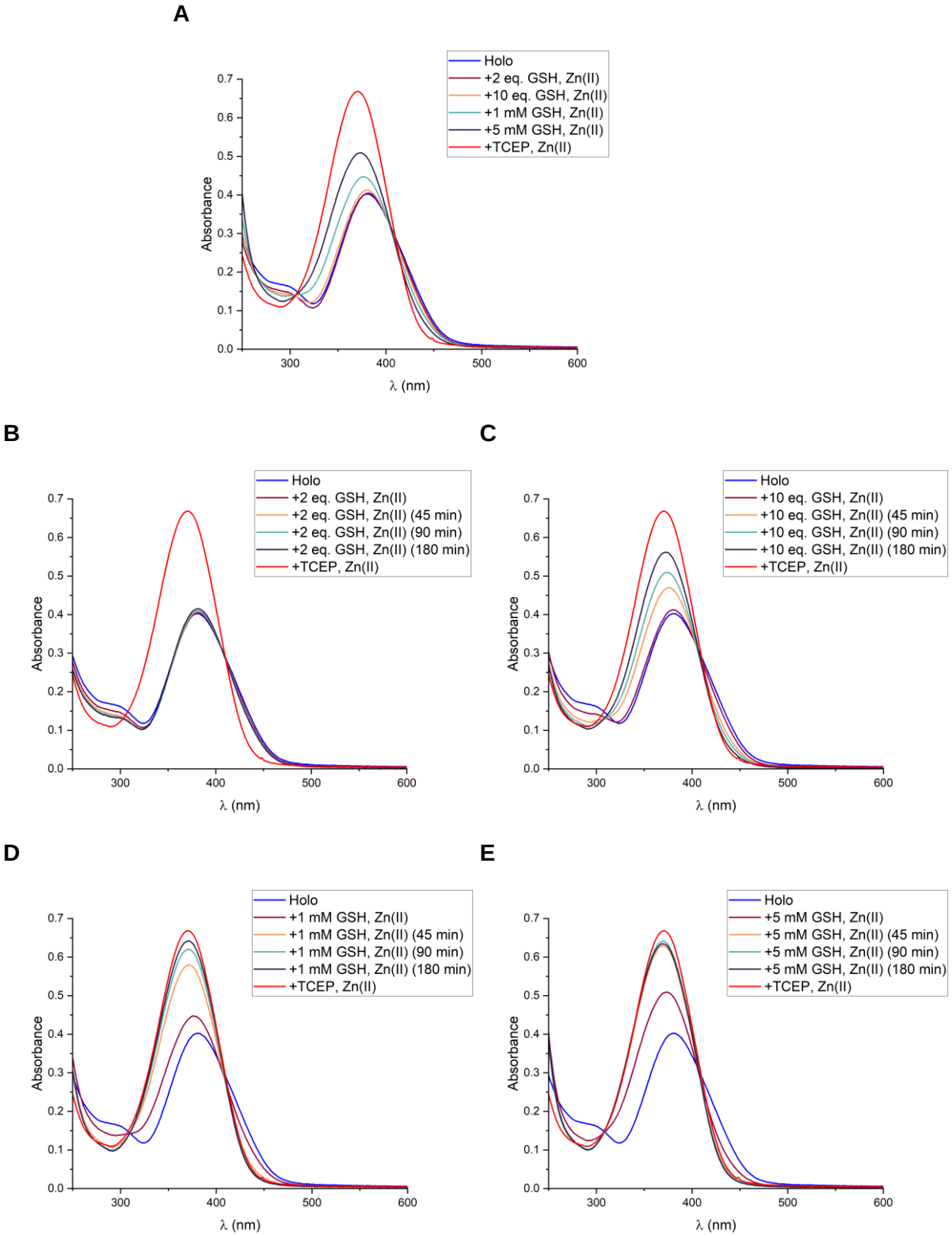

Fig. S12. Zn(II) coordination of Holo mediated by GSH. (A) Holo was incubated with Zn(II) in the presence of GSH. Zn(II) coordination by Holo in the presence of 2 eq. (B), 10 eq. (C), 1 mM (D), or 5 mM GSH (E) was monitored over time. The assay was performed with 50 µM Holo, 0.5 eq. Zn(II), and the specified amount of GSH in 75 mM Tris-HCl, pH 7.4. The spectrum of the complex of Holo reduced with TCEP is included for comparison. Data of (A) and (D) is also shown in Fig. 4 in the main text, but included here to ease comparison.

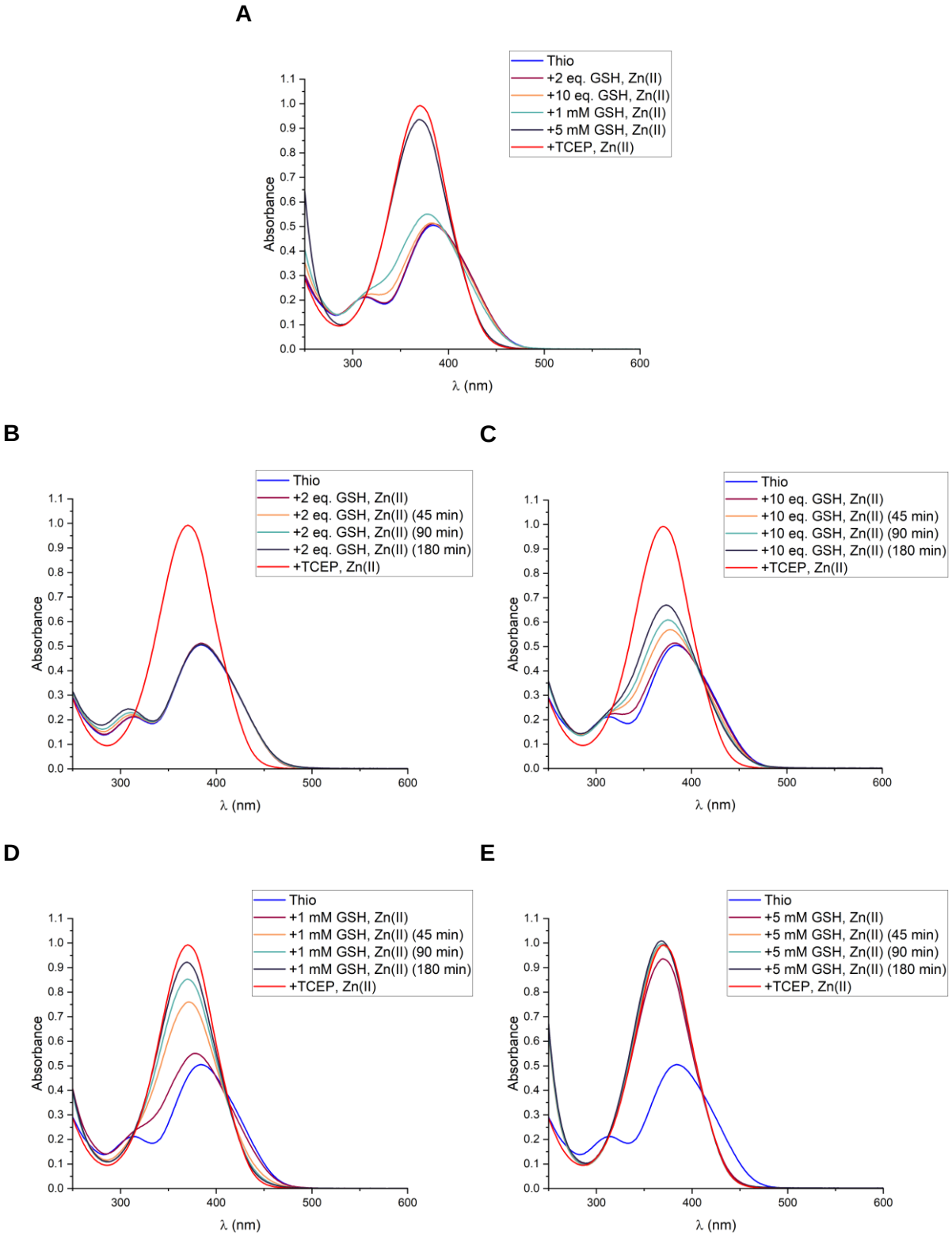

Fig. S13. Zn(II) coordination of thiolutin mediated by GSH. (A) Thiolutin was incubated with Zn(II) in the presence of GSH. Zn(II) coordination by thiolutin in the presence of 2 eq. (B), 10 eq. (C), 1 mM (D), or 5 mM GSH (E) was monitored over time. The assay was performed with 50 µM thiolutin, 0.5 eq. Zn(II), and the specified amount of GSH in 75 mM Tris-HCl, pH 7.4. The spectrum of the complex of thiolutin reduced with TCEP is included for comparison. Data of (A) is also shown in Fig. 4 in the main text, but included here to ease comparison.

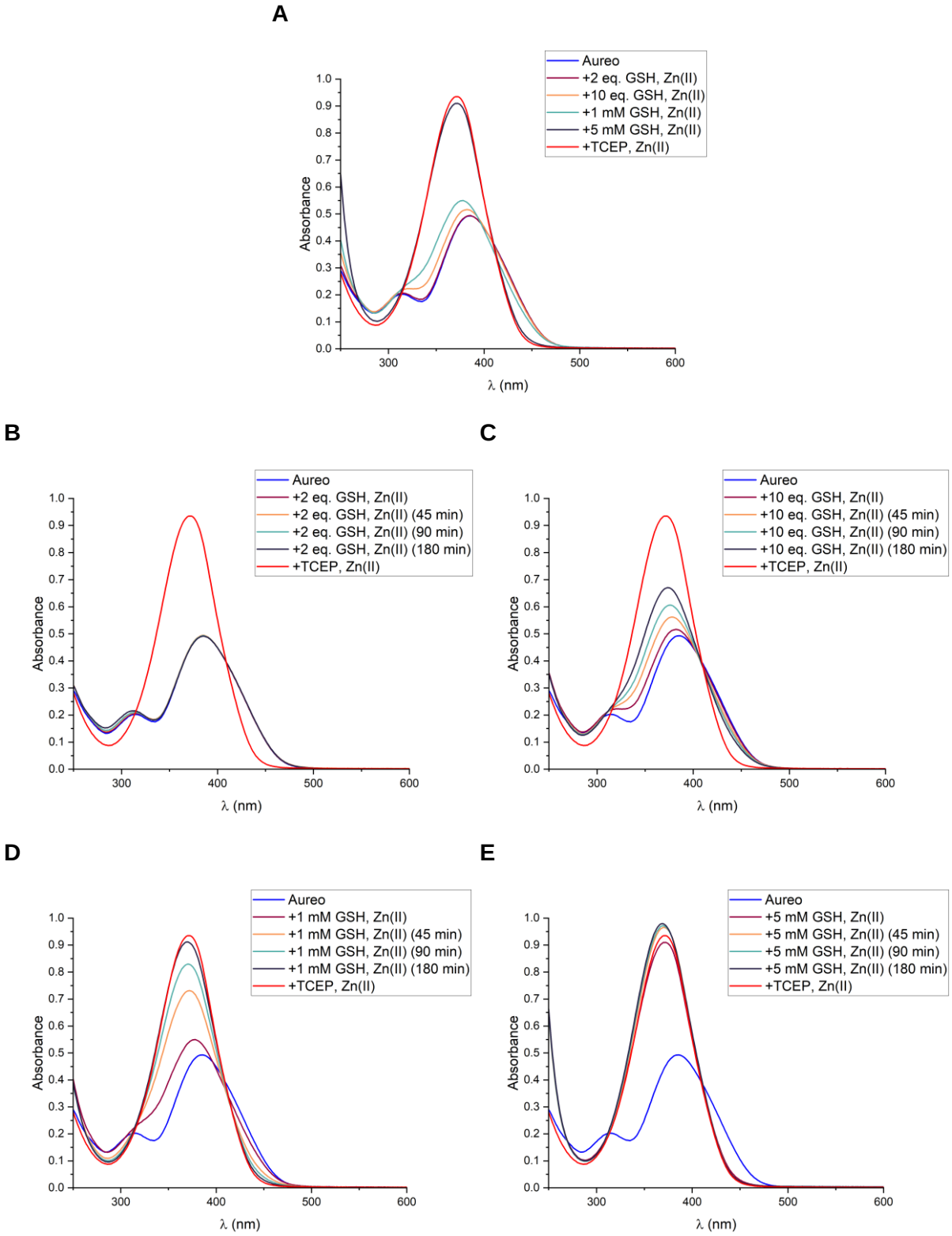

Fig. S14. Zn(II) coordination of aureothricin mediated by GSH. (A) Aureothricin was incubated with Zn(II) in the presence of GSH. Zn(II) coordination by aureothricin in the presence of 2 eq. (B), 10 eq. (C), 1 mM (D), or 5 mM GSH (E) was monitored over time. The assay was performed with 50 µM aureothricin, 0.5 eq. Zn(II), and the specified amount of GSH in 75 mM Tris-HCl, pH 7.4. The spectrum of the complex of aureothricin reduced with TCEP is included for comparison. Data of (A) is also shown in Fig. 4 in the main text, but included for comparison

3) Redox Equilibration Assays

3.1) Compound chromatograms

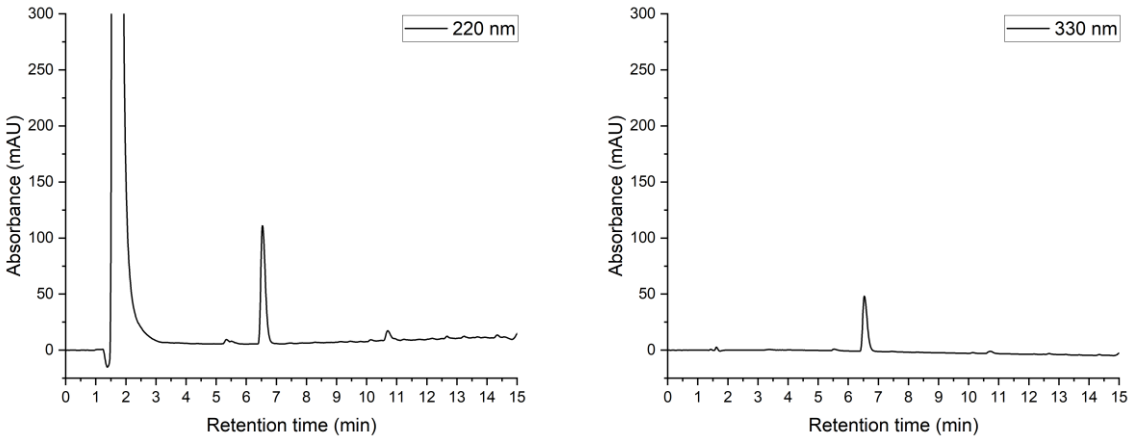

Fig. S15. Analytical HPLC traces of Holo (1 mM); absorbance monitored at 220 nm and 330 nm.

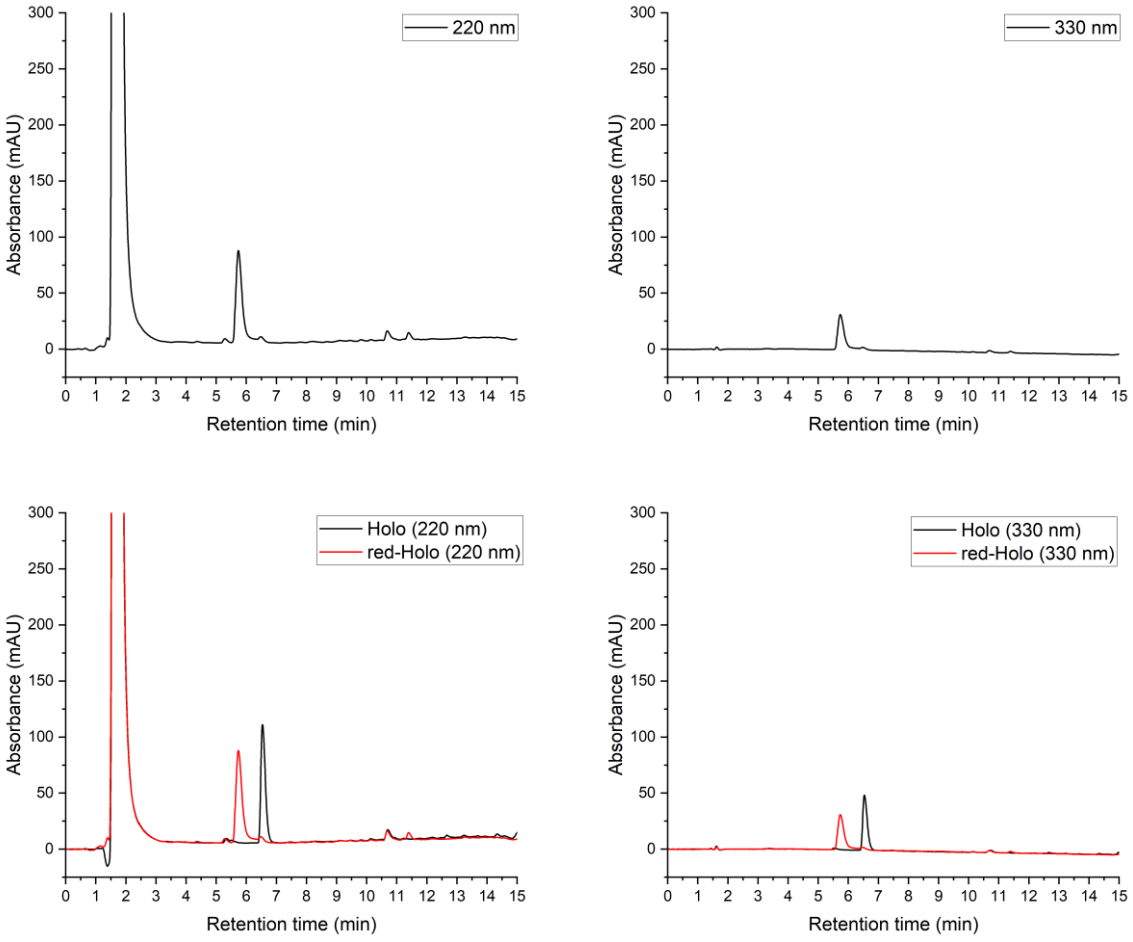

Fig. S16. Analytical HPLC traces of *red*-Holo (reduced with 10 eq. TCEP); absorbance monitored at 220 nm and 330 nm. Also shown is an overlay of the traces with those of Holo.

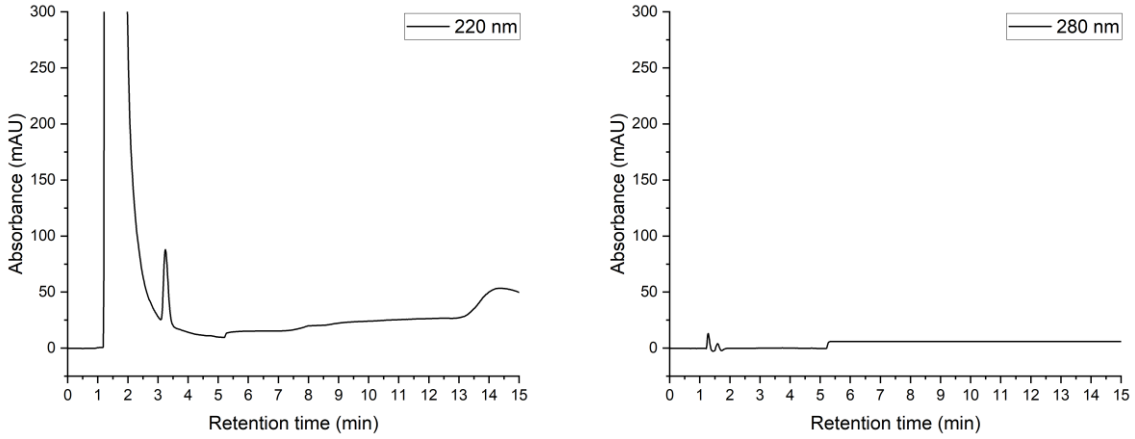

Fig. S17. Analytical HPLC traces of DTT (5 mM); absorbance monitored at 220 nm and 280 nm.

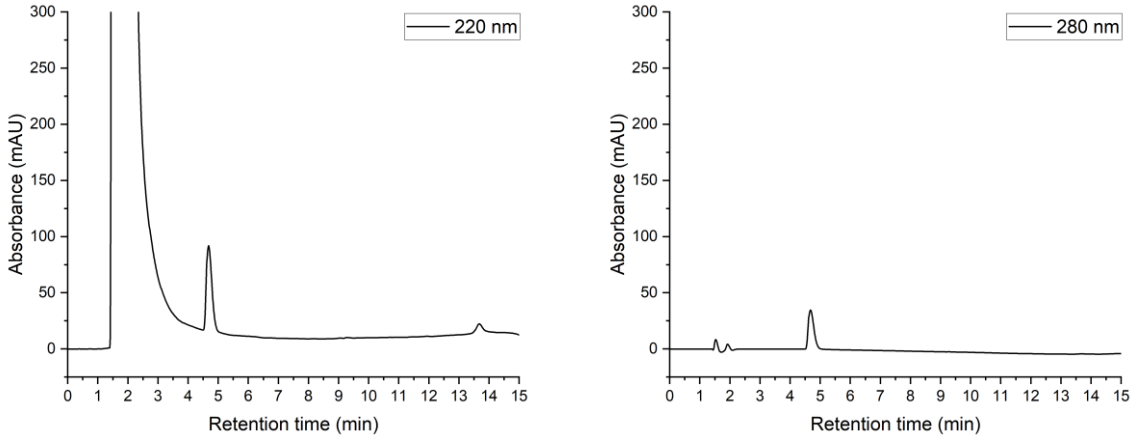

Fig. S18. Analytical HPLC traces of DTT_{ox} (5 mM); absorbance monitored at 220 nm and 280 nm.

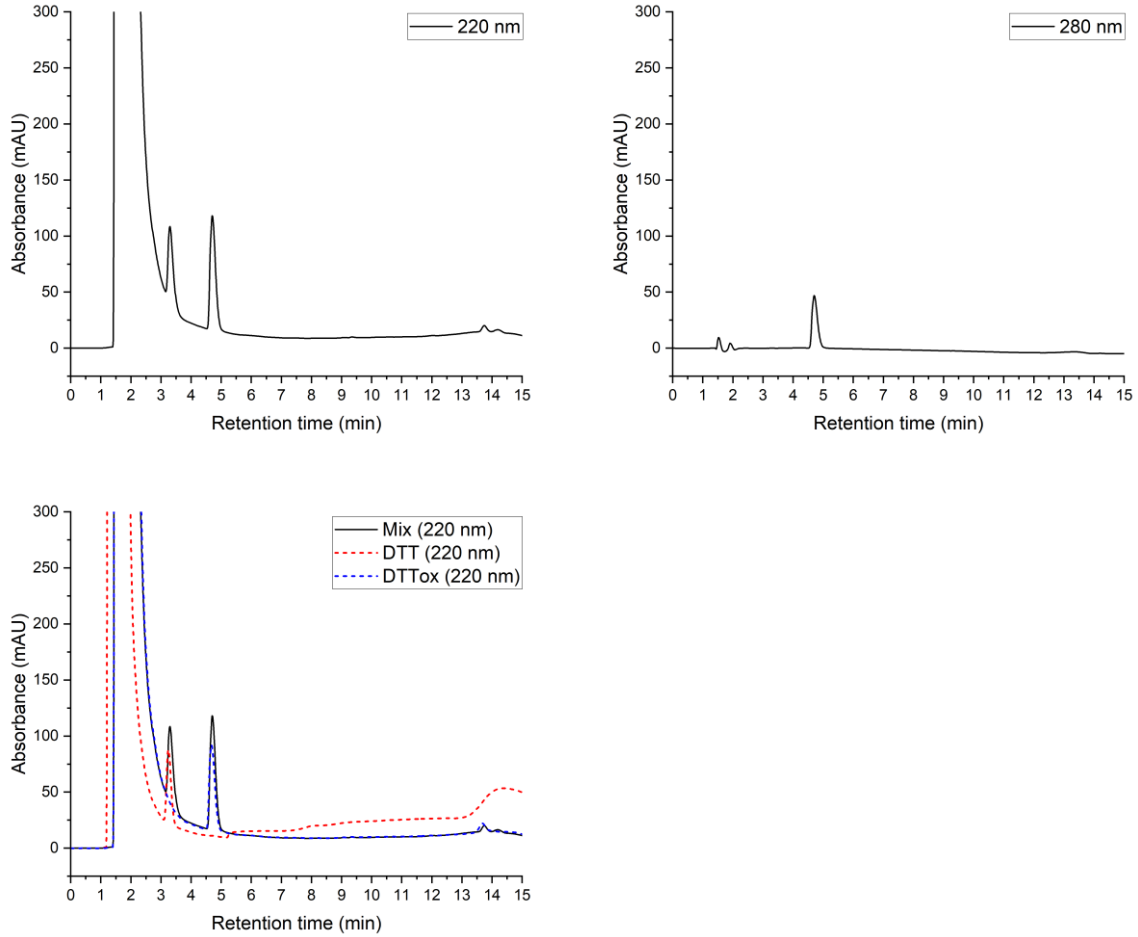

Fig. S19. Analytical HPLC traces of a mixture of DTT and DTT_{ox} (5 mM each); absorbance monitored at 220 nm and 280 nm.

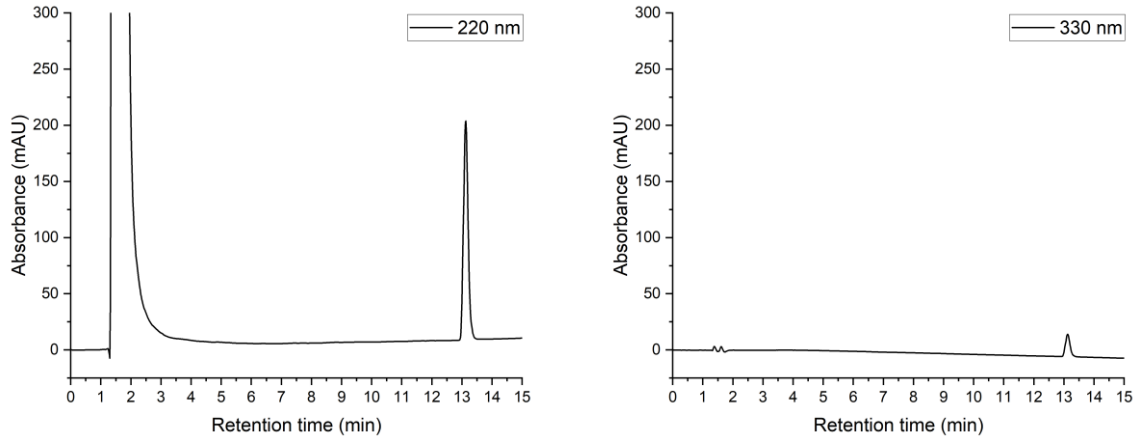

Fig. S20. Analytical HPLC traces of LA (5 mM); absorbance monitored at 220 nm and 330 nm.

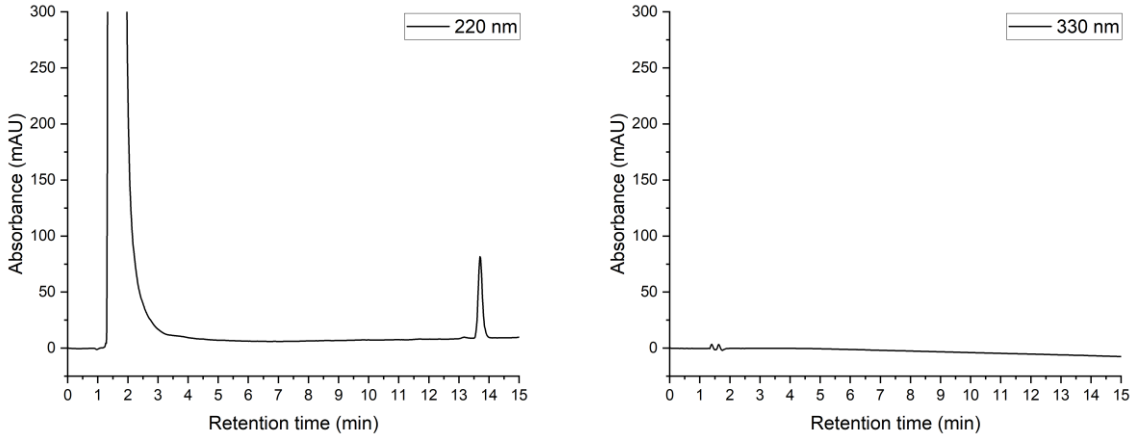

Fig. S21. Analytical HPLC traces of DHLA (5 mM); absorbance monitored at 220 nm and 330 nm.

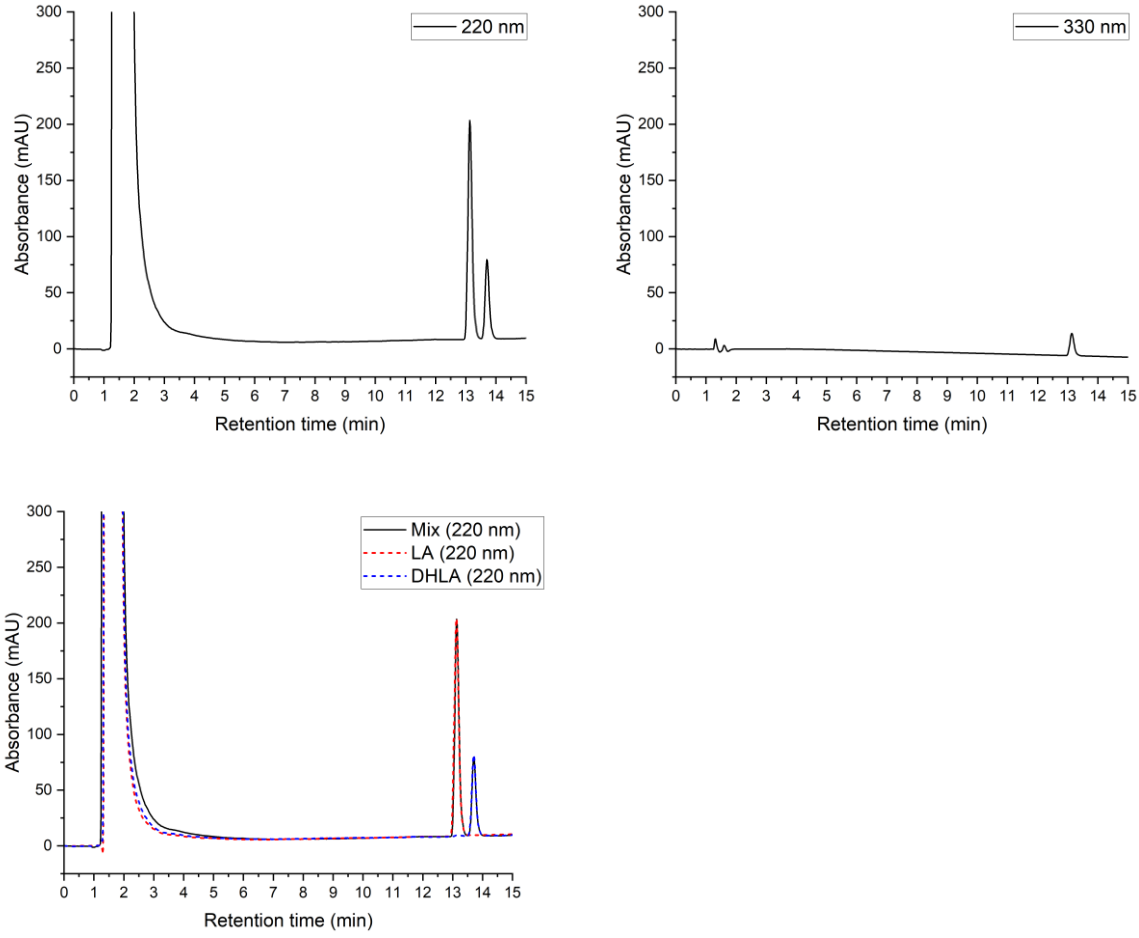

Fig. S22. Analytical HPLC traces of a mixture of LA and DHLA (5 mM each); absorbance monitored at 220 nm and 330 nm.

3.2) Equilibration with DTT and DTT_{ox}

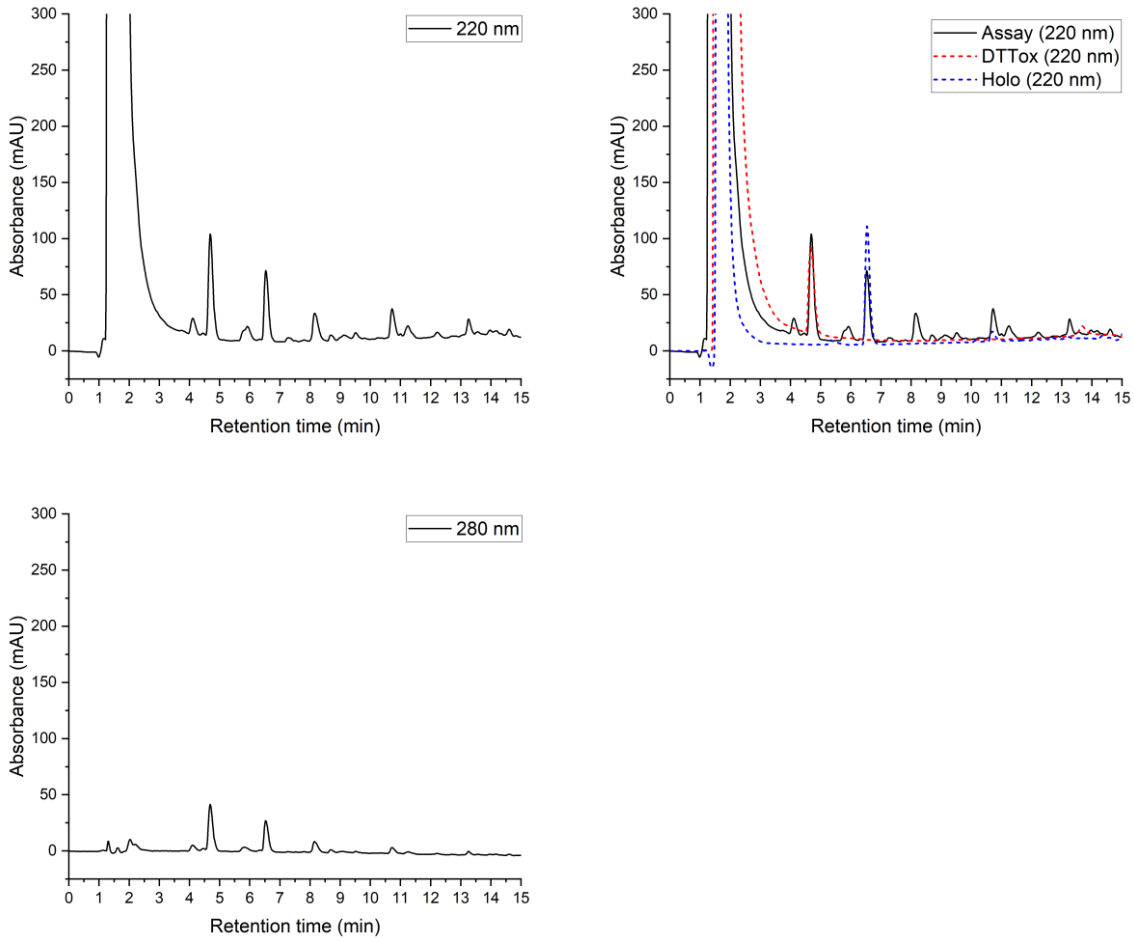

Fig. S23. Equilibration of Holo with DTT. Analytical HPLC traces of the assay; absorbance monitored at 220 nm and 280 nm. 5 mM Holo were incubated with 5 mM DTT in 75 mM Tris-HCl, pH 7.4 for 1 d under an N_2 atmosphere.

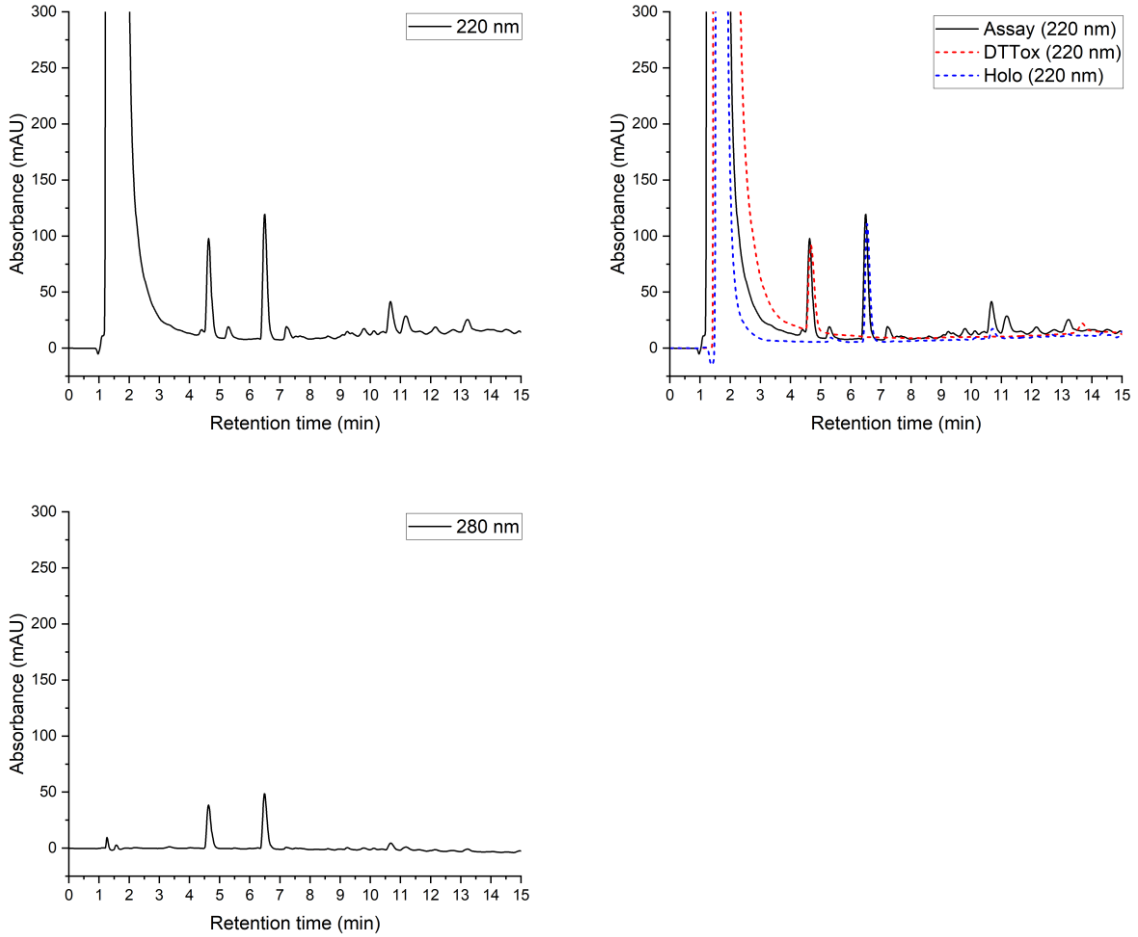

Fig. S24. Equilibration of *red*-Holo with DTT_{ox}. Analytical HPLC traces of the assay; absorbance monitored at 220 nm and 280 nm. 5 mM *red*-Holo (reduced with 1 eq. TCEP) were incubated with 5 mM DTT in 75 mM Tris-HCl, pH 7.4 for 1 d under an N_2 atmosphere.

3.3) Equilibration with DHLA and LA

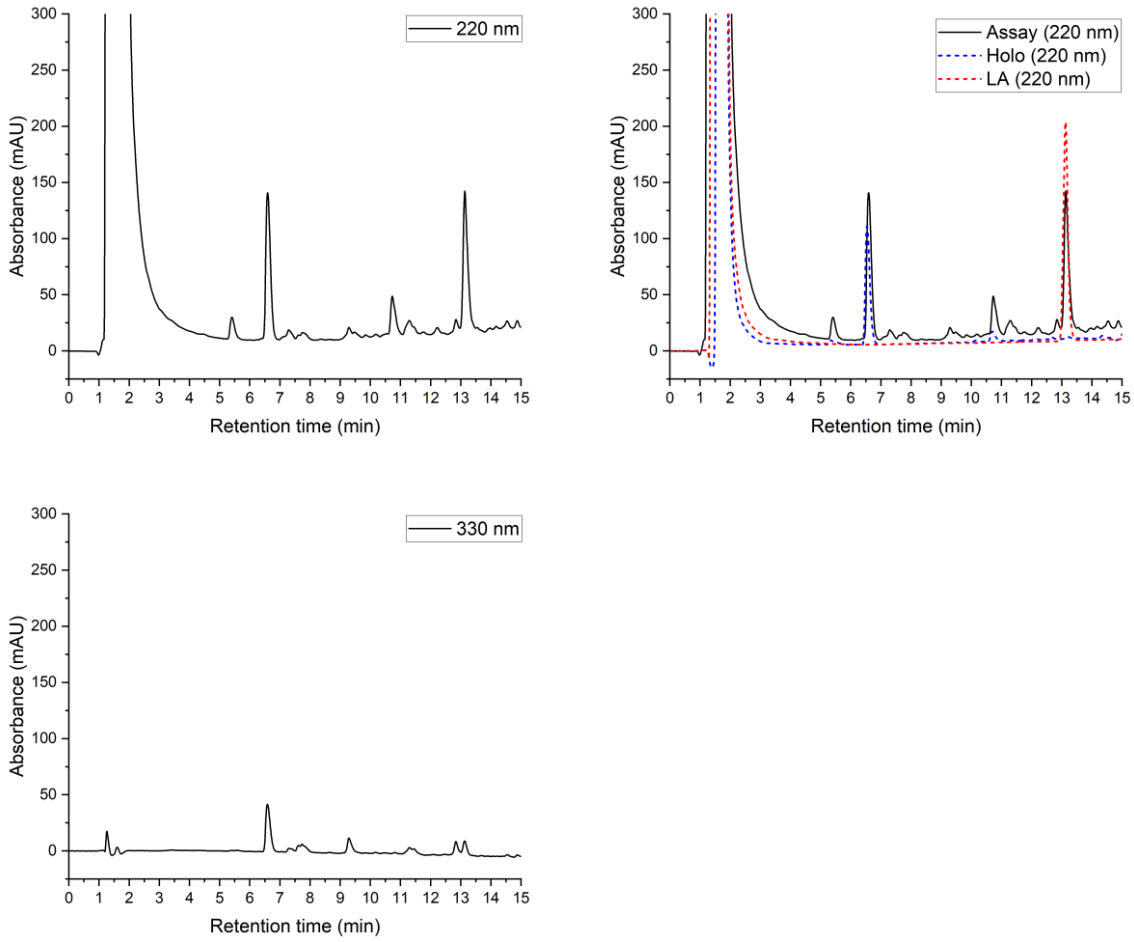

Fig. S25. Equilibration of Holo with DHLA. Analytical HPLC traces of the assay; absorbance monitored at 220 nm and 330 nm. 5 mM Holo were incubated with 5 mM DHLA in 75 mM Tris-HCl, pH 7.4 for 1 d under an N_2 atmosphere.

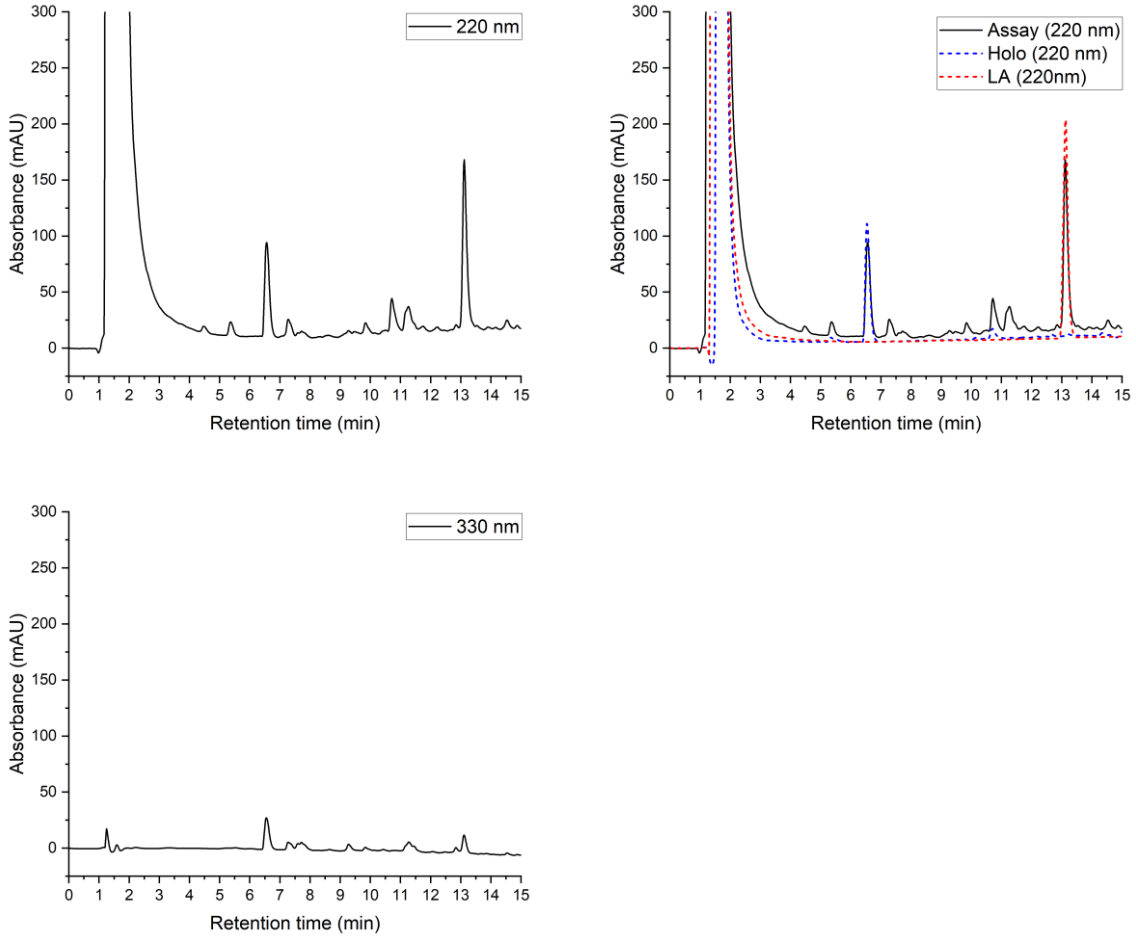

Fig. S26. Equilibration of *red*-Holo with LA. Analytical HPLC traces of the assay; absorbance monitored at 220 nm and 330 nm. 5 mM *red*-Holo (reduced with 1 eq. TCEP) were incubated with 5 mM LA in 75 mM Tris-HCl, pH 7.4 for 1 d under an N_2 atmosphere.

3.4) Equilibration of DTT and LA

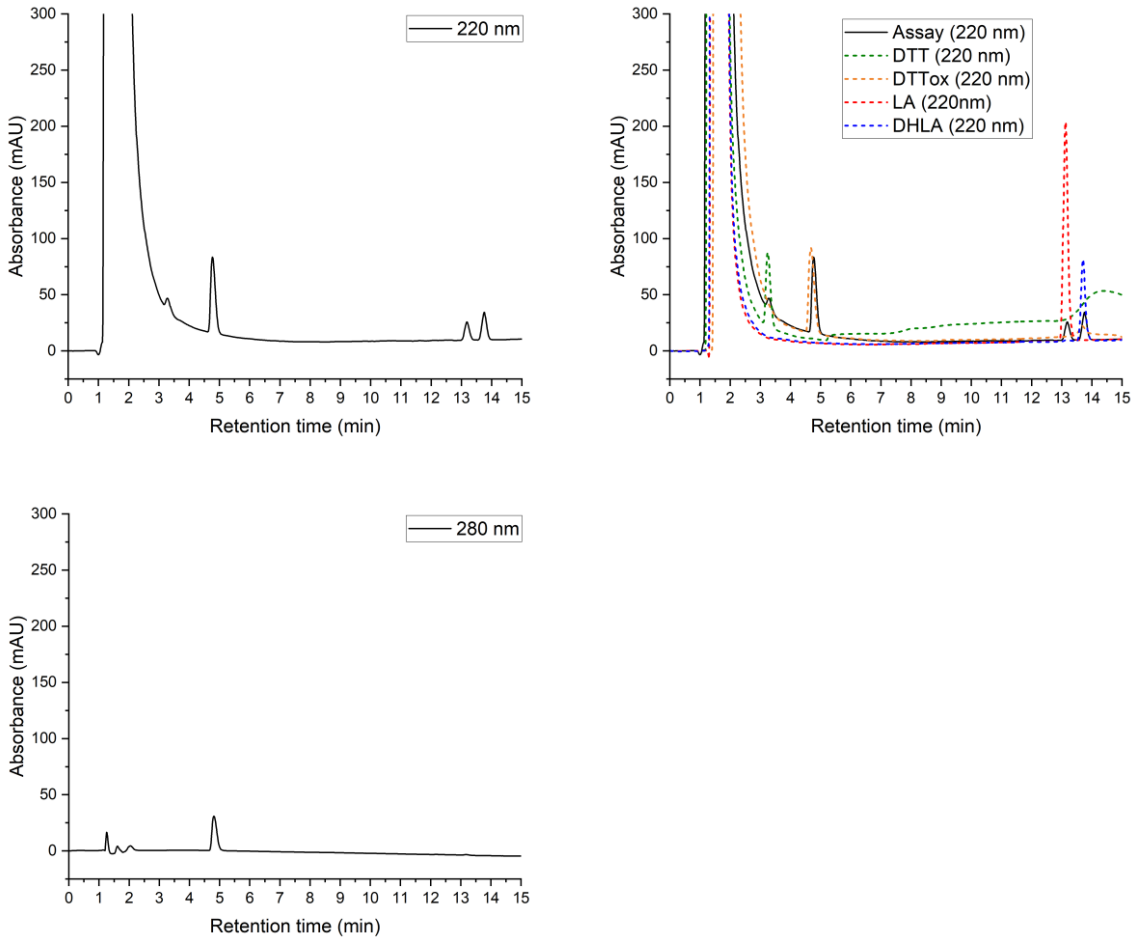

Fig. S27. Equilibration of LA with DTT. Analytical HPLC traces of the assay; absorbance monitored at 220 nm and 280 nm. 5 mM LA were incubated with 5 mM DTT in 75 mM Tris-HCl, pH 7.4 for 1 d under an N_2 atmosphere.

4) Cyclic Voltammetry

4.1) Tris buffer

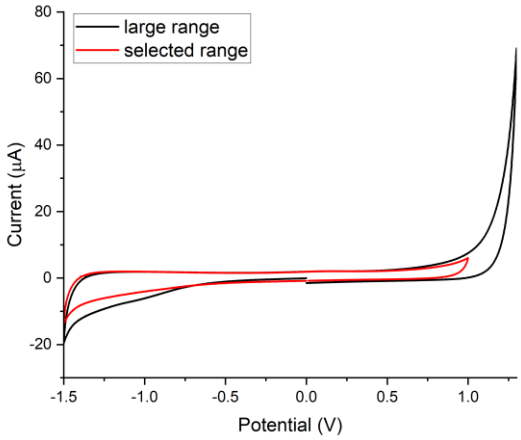

Fig. S28. CV of the employed Tris buffer (background scan). The measurements were performed in 1 M KCl, 75 mM Tris-HCl, pH 7.4, at a glassy carbon electrode. The potential range colored in red was used for the measurements with Holo, GSSG and LA.

4.2) Holo

Detailed discussion of the cyclic voltammograms

Overview. The voltammogram of Holo displays three irreversible peaks (Fig. S29A). The irreversible cathodic peak likely originates from an electron transfer onto the disulfide, resulting in cleavage of the S–S bond and formation of the dithiolate (Scheme S2). The anodic peak at lower potential (oxidation-I) likely results from the oxidation of the thiolates to S radicals, which combine intramolecularly under back formation of the disulfide. The anodic peak at higher potential (oxidation-II) is probably caused by an oxidation of the disulfide to a thiosulfinate. The irreversibility of the electron transfers is confirmed by changes in the peak potentials that are observed upon an increase of the scan rate (Fig. S30).

Interconnection between reduction and oxidation peaks. Both oxidative processes are interconnected with the broad reduction peak. If both oxidation peaks are passed during the measurement, the intensity of the reduction peak stays about constant over the course of several scans (Fig. S29A). If only oxidation-I is passed, the intensity of the reduction peak decreases significantly (Fig. S29B). Thus, oxidation-II also seems to contribute molecules for the reduction. If no oxidation is passed (Fig. S29E), the intensity of the reduction peak decreases as well, but not much further than when oxidation-I is passed (Fig. S29B). This indicates that the molecules from both oxidations are reduced within the broad reduction peak.

Interestingly, the intensity of the reduction peak does not vanish if no oxidation is passed (Fig. S29E), indicating that some molecules are chemically oxidized. Possibly, the large excess of Holo disulfide in the solution mediates a fast chemical oxidation, which correlates with the high oxidation sensitivity of the dithiol. Such simultaneous chemical oxidation may also explain the relatively low peak intensity of oxidation-I.

If the scan is started with an anodic scan, oxidation-I is not detectable during the first scan (Fig. S29C). Oxidation-I only appears after the reduction has been passed. This indicates that the reduction generates the dithiol, which is then oxidized back to the disulfide during oxidation-I. In contrast to oxidation-I, oxidation-II is detectable even if the reduction has not been passed before (Fig. S29D). This indicates that the molecules in solution, namely the Holo disulfide, is oxidized during that reaction, possibly under formation of thiosulfinates. If the reduction is not passed (Fig. S29F), the peak intensity of oxidation-II decreases significantly, indicating that the reduction peak also reduces the species formed during oxidation-II.

Overall, it seems that the broad reduction peak covers the reduction of both the Holo disulfide (from oxidation-I) and the oxidized disulfide (poss. thiosulfinate, from oxidation-II).

Impact of chemical reduction. If Holo is chemically reduced (with TCEP) to *red*-Holo (Fig. S31A), the reduction peak is not detectable during the first scan, confirming that the chemical and electrochemical reductions generate the same species. The reduction peak is detectable after the oxidation has been passed (Fig. S31A, S31B). However, the intensity of the reduction peak of the *red*-Holo sample (Fig. S31A, S31B) is much lower than that of the Holo sample (Fig. S29A). This again may indicate a fast exchange with the main solution; the large excess of *red*-Holo may mediate a chemical reduction of the formed oxidized species.
In the case of the *red*-Holo sample (Fig. S31A), the intensity of the oxidation-I peak is much higher than for the Holo sample (Fig. S29A). This is likely due to the high concentration of *red*-Holo in the solution and consistent with the oxidation of the thiol. In contrast, the peak intensities of oxidation-II are similar for the Holo (Fig. S29A) and the *red*-Holo sample (Fig. S31A), consistent with the oxidation of the Holo disulfide. If only oxidation-I is passed, the intensity of the reduction peak is again less intense than when oxidation-II was also passed (Fig. S31C), similar to the Holo sample (Fig. S29C, S29D). This confirms that the reduction peak covers the reduction of both oxidized species.

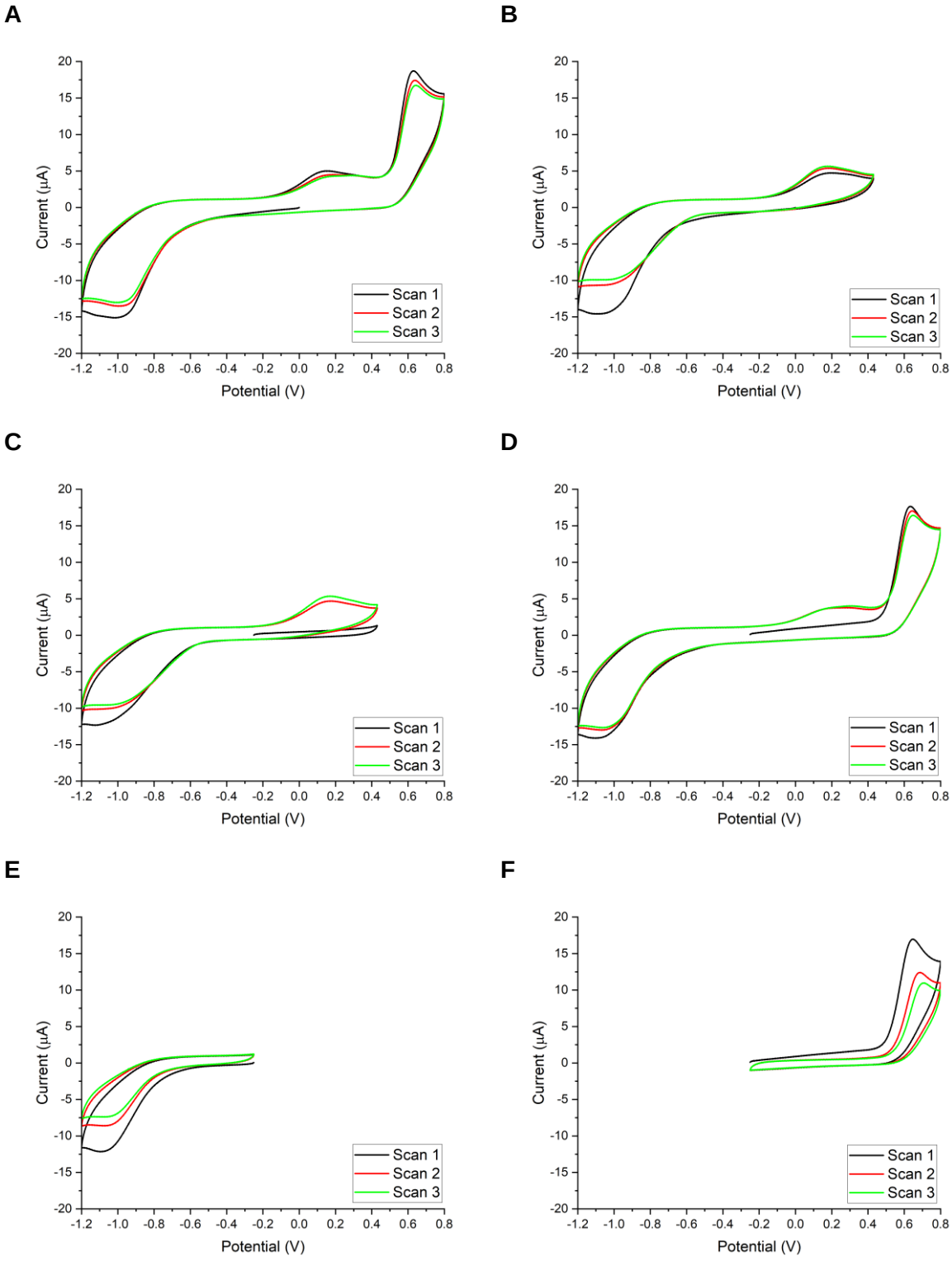

Fig. S29. CV of Holo. (A) Reduction and both oxidation peaks; measurement started with cathodic scan. (B) Reduction and 1st oxidation peak; measurement started with cathodic scan. (C) Reduction and 1st oxidation peak; measurement started with anodic scan. (D) Reduction and both oxidations; measurement started with anodic scan. (E) Reduction; measurement started with cathodic scan. (F) Oxidations; measurement started with anodic scan. The measurements were performed with 1 mM Holo in 75 mM Tris-HCl, pH 7.4. Data of (A) is also shown in Fig. 3 in the main text, but included here to ease comparison.

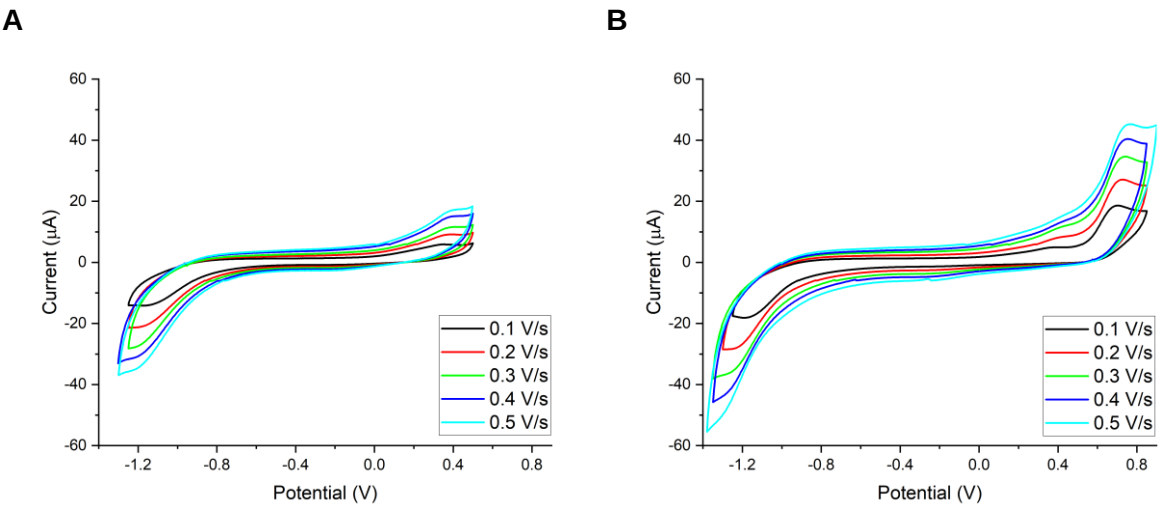

Fig. S30. CV of Holo at different scan rates. (A) Reduction and 1st oxidation peak. (B) Reduction and both oxidation peaks. Measurements started with cathodic scan. The measurements were performed with 1 mM Holo in 75 mM Tris-HCl, pH 7.4, and the scan rate was varied between 0.1–0.5 V/s.

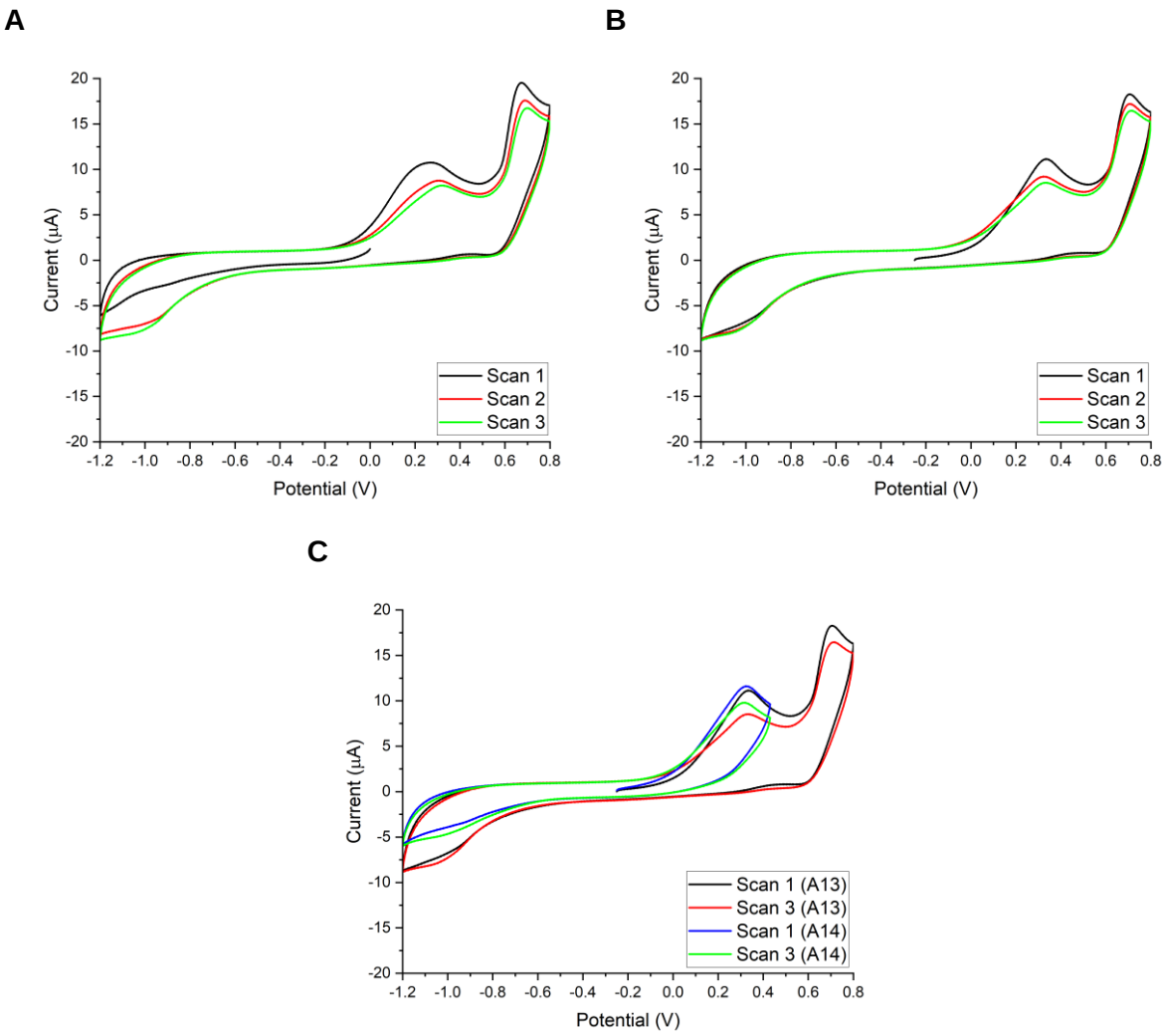

Fig. S31. CV of *red*-Holo. (A) Reduction and both oxidation peaks; measurement started with cathodic scan. (B) Reduction and both oxidation peaks; measurement started with anodic scan. (C) Comparison of measurements that covered the range with both oxidation peaks or only the 1st oxidation peak; measurements started with anodic scan. The measurements were performed with 1 mM *red*-Holo (reduced with 1 eq. TCEP) in 75 mM Tris-HCl, pH 7.4.

4.3) GSSG

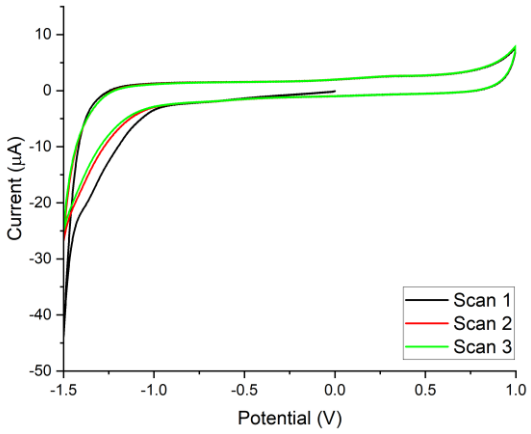

Fig. S32. CV of GSSG. The measurement was performed with 5 mM GSSG in 75 mM Tris-HCl, pH 7.4. The measurement was started with the cathodic scan. The reduction peak is only detectable during Scan-1 due to the irreversible cleavage of the disulfide bond under release of GSH. Some of the data is also shown in Fig. 3 in the main text, but included here to ease comparison.

4.4) LA

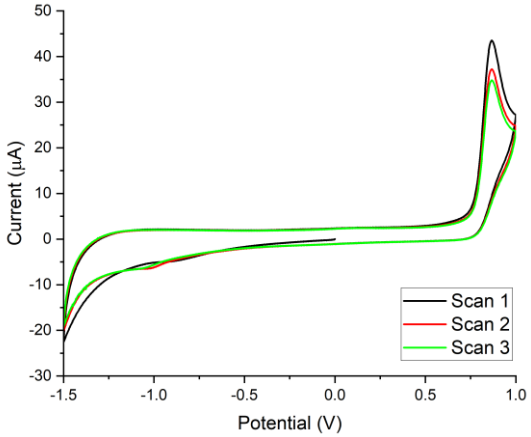

Fig. S33. CV of LA. The measurement was performed with 1 mM LA in 75 mM Tris-HCl, pH 7.4. The measurement was started with the cathodic scan. No peak for the reduction of the disulfide was detectable within the accessible potential range. The intense oxidation peak likely results from the formation of the thiosulfinate.

5) NMR Spectra

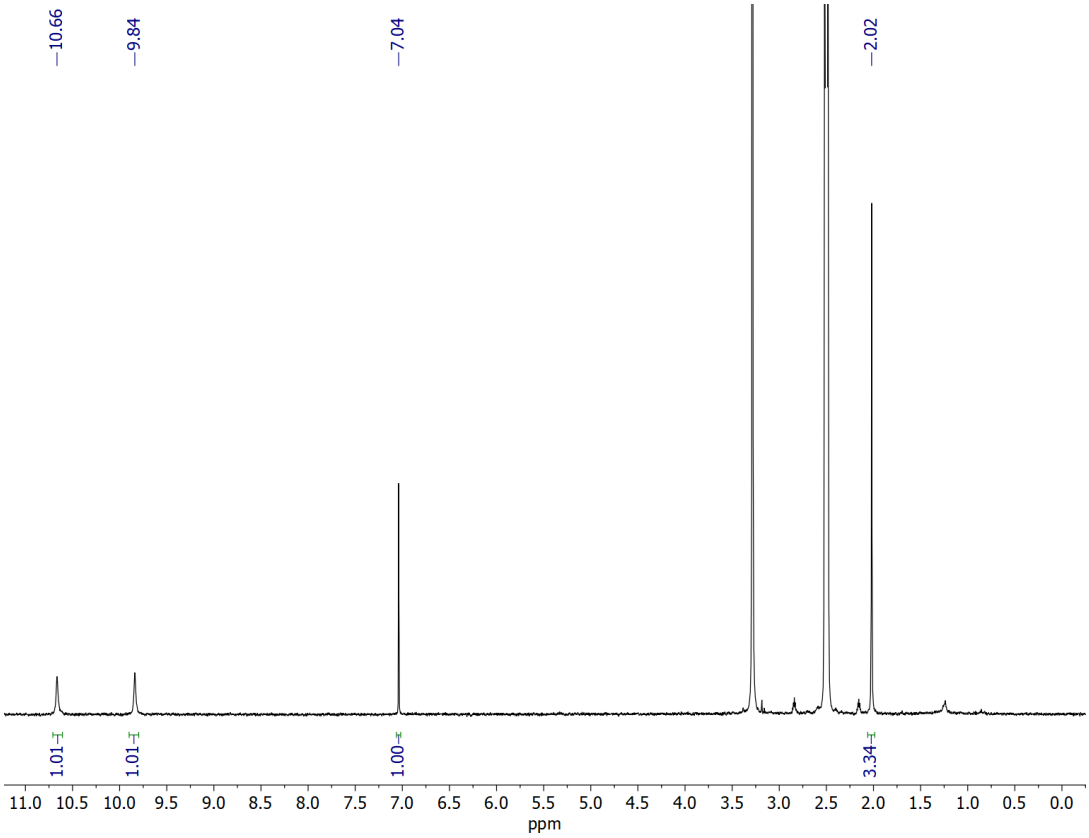

Fig. S34. ^{1}H NMR of Holo (**1**) (DMSO-d_6, 200 MHz).

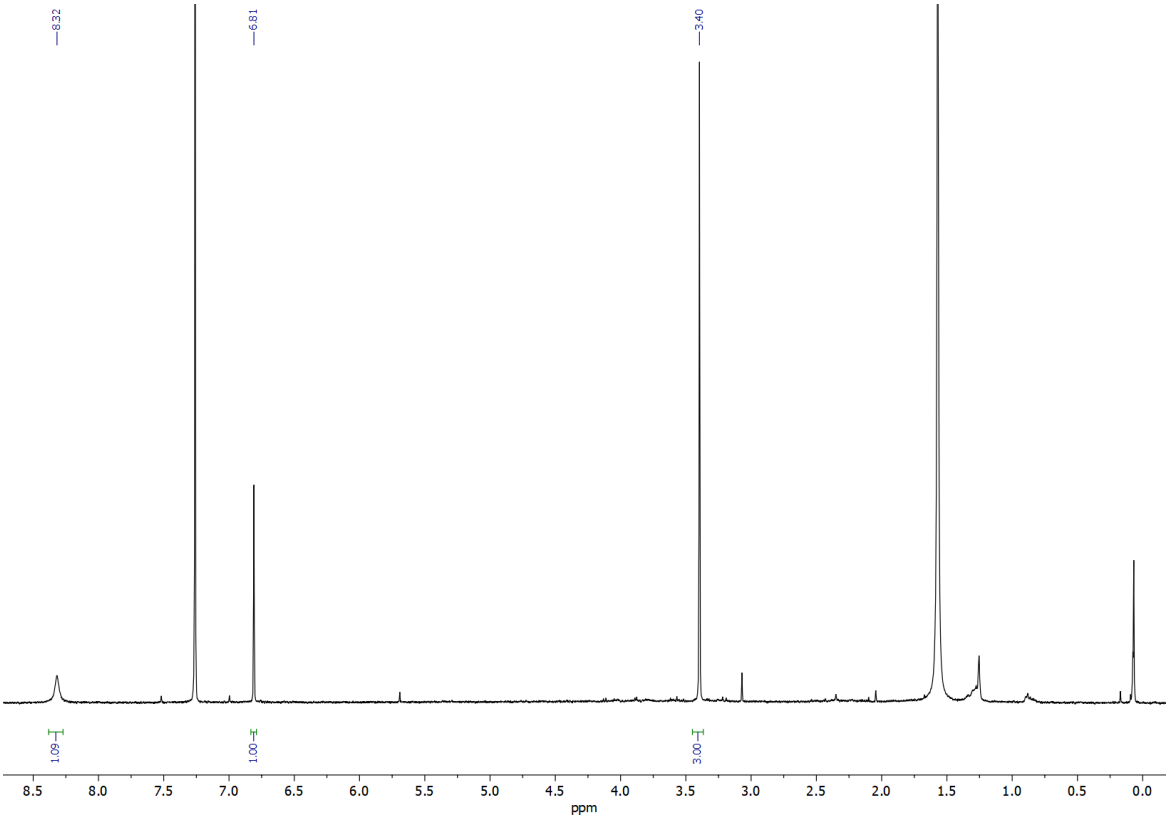

Fig. S35. ^{1}H NMR of CF_3-thiolutin (**9**) ($CDCl_3$, 400 MHz).

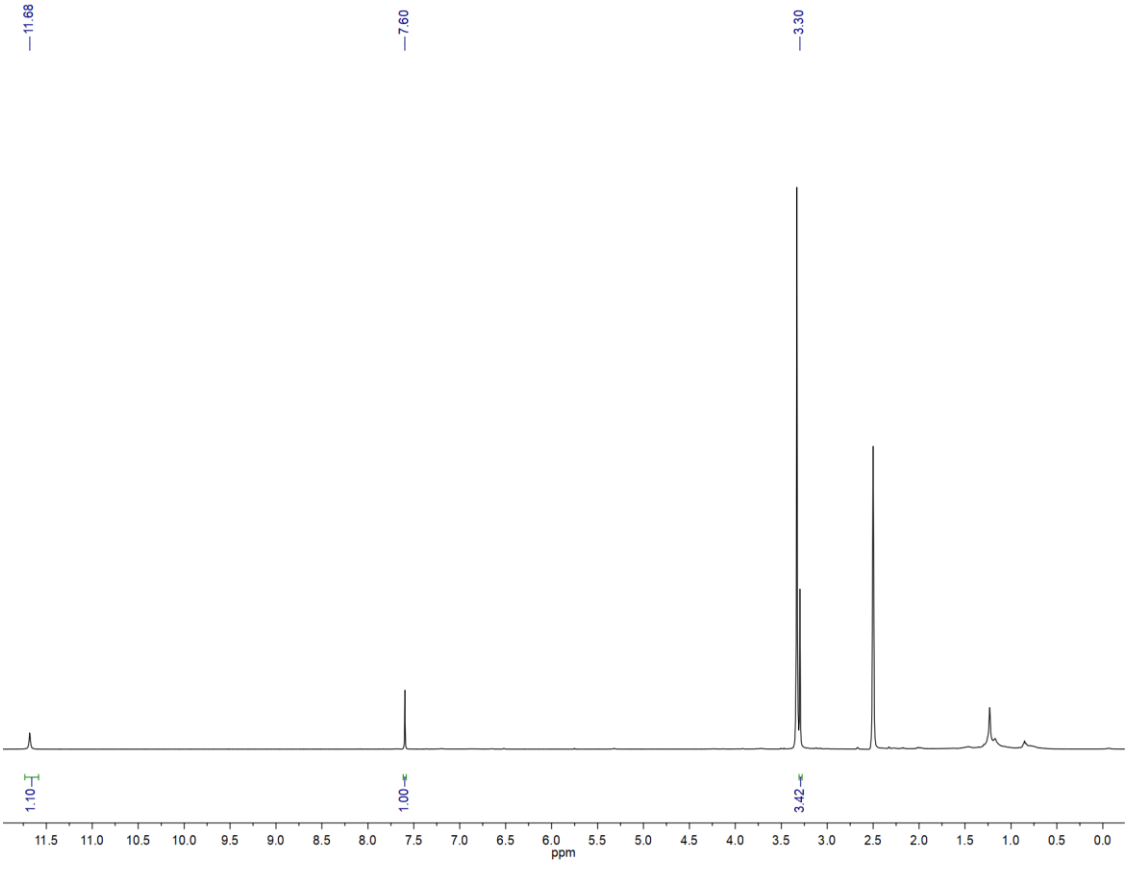

Fig. S36. ^{1}H NMR of CF_3-thiolutin (**9**) (DMSO-d_6, 400 MHz).

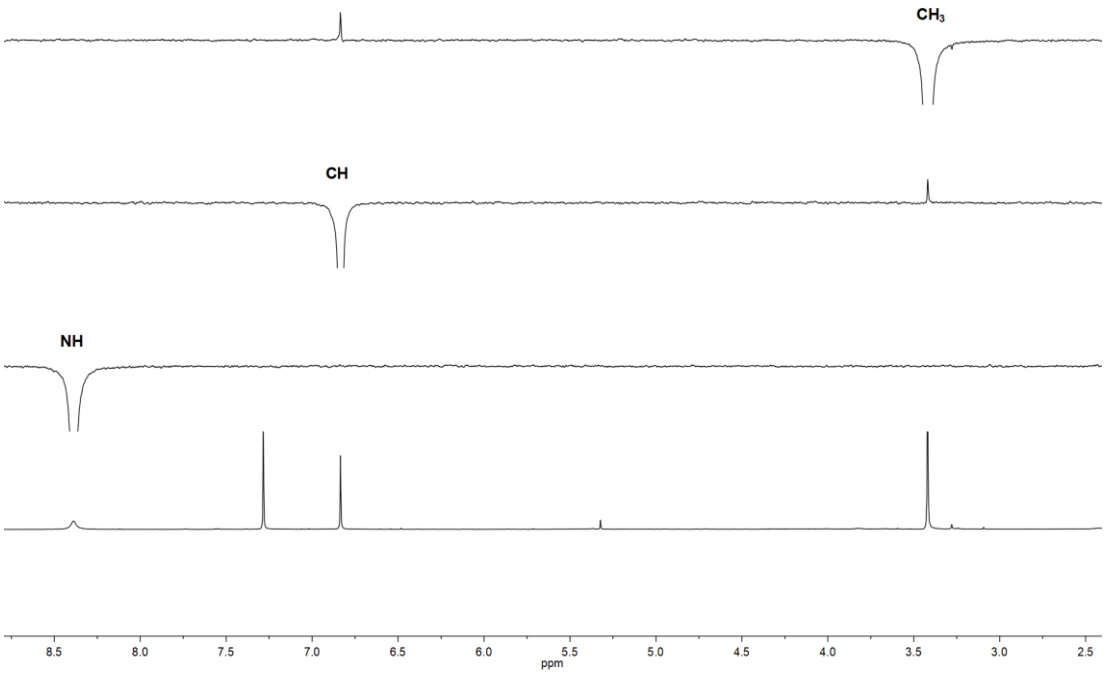

Fig. S37. Selective 1D-NOESY NMR of CF_3-thiolutin (**9**) ($CDCl_3$, 400 MHz); ^1H NMR at bottom.

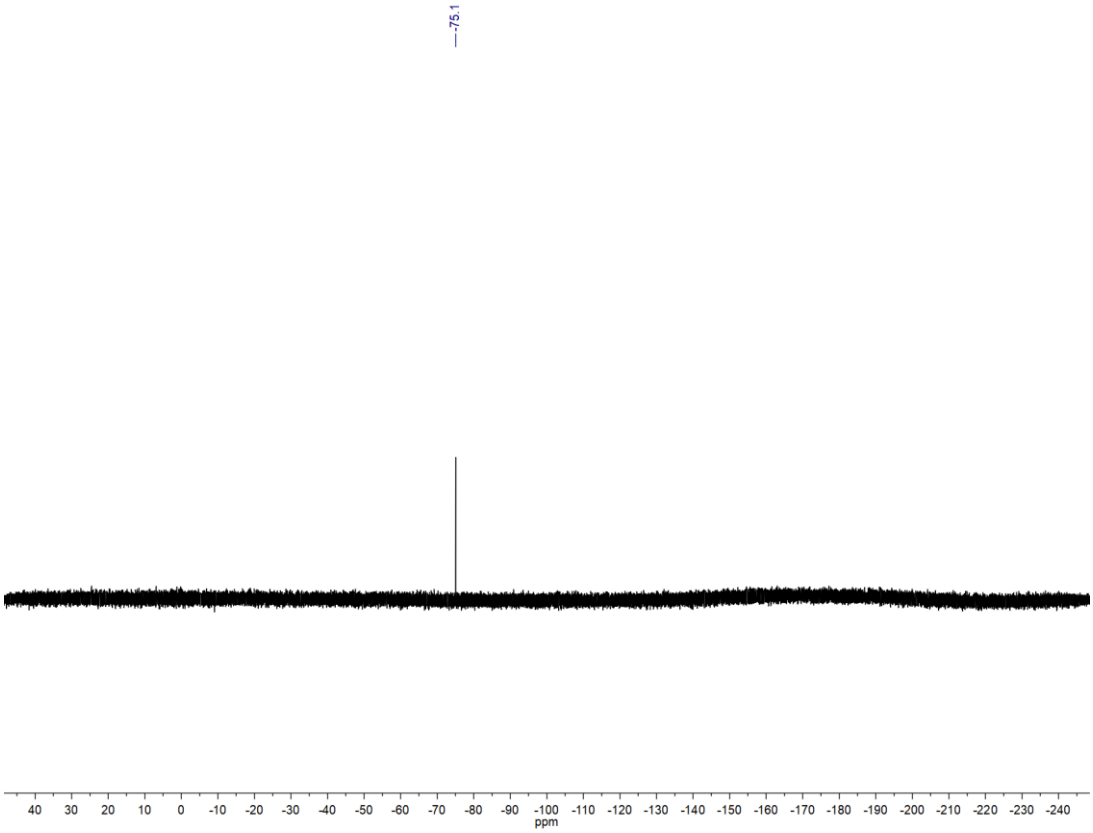

Fig. S38. ^{19}F NMR of CF_3-thiolutin (**9**) ($CDCl_3$, 235 MHz).

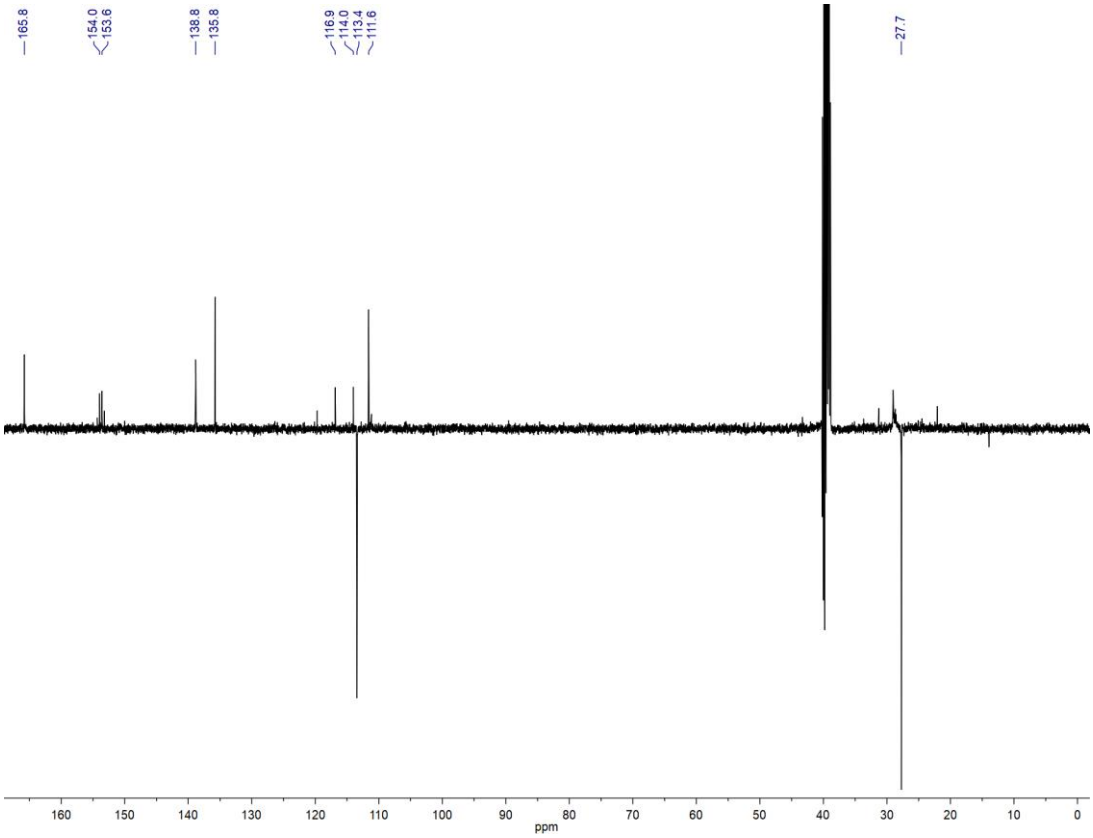

Fig. S39. $^{13}C\{^{1}H\}$ NMR of CF_3-thiolutin (**9**) (DMSO-d_6, 100 MHz).

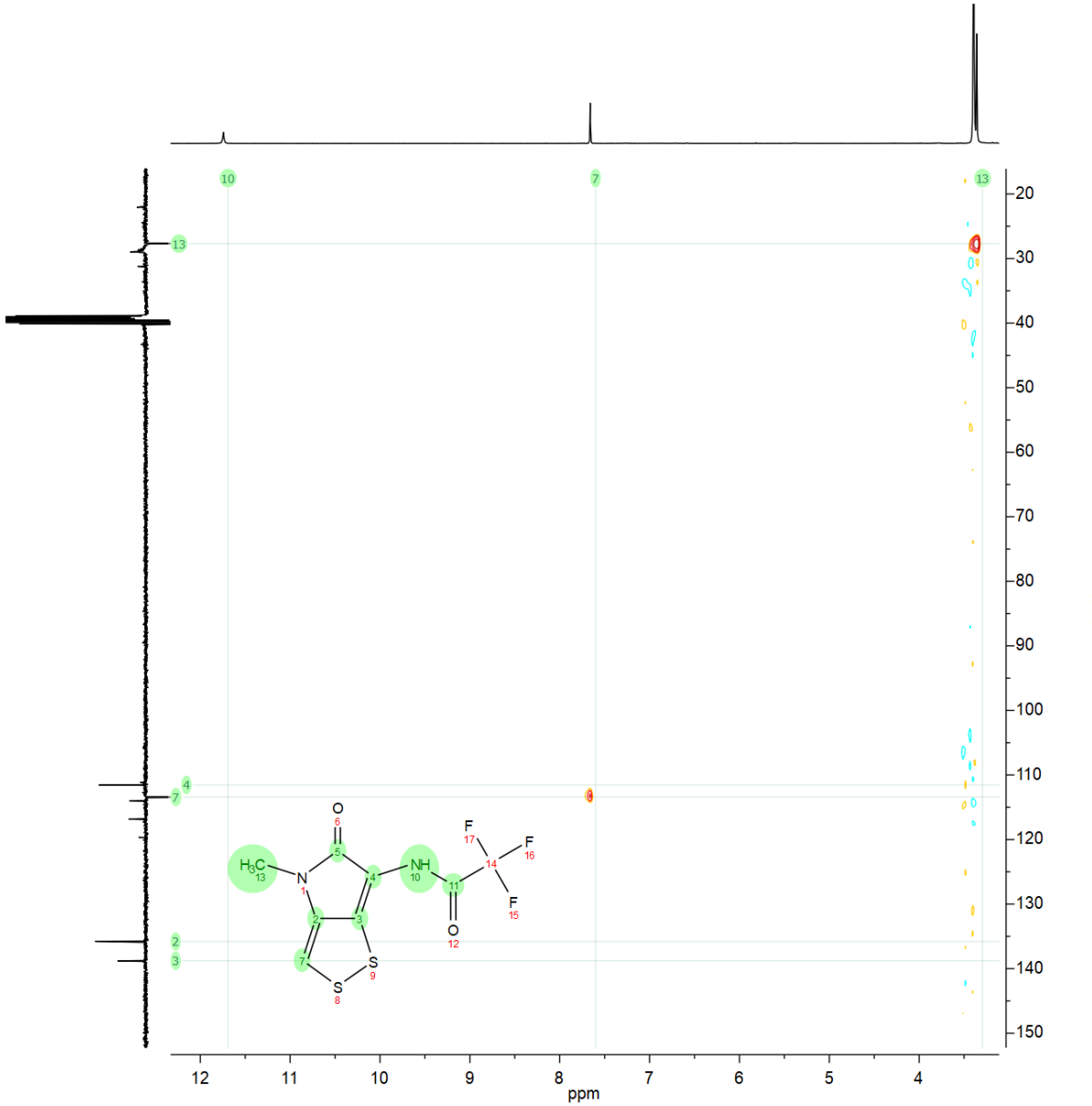

Fig. S40. (^{1}H,^{13}C)-HSQC NMR of CF_3-thiolutin (**9**) (DMSO-d_6, 400 MHz).

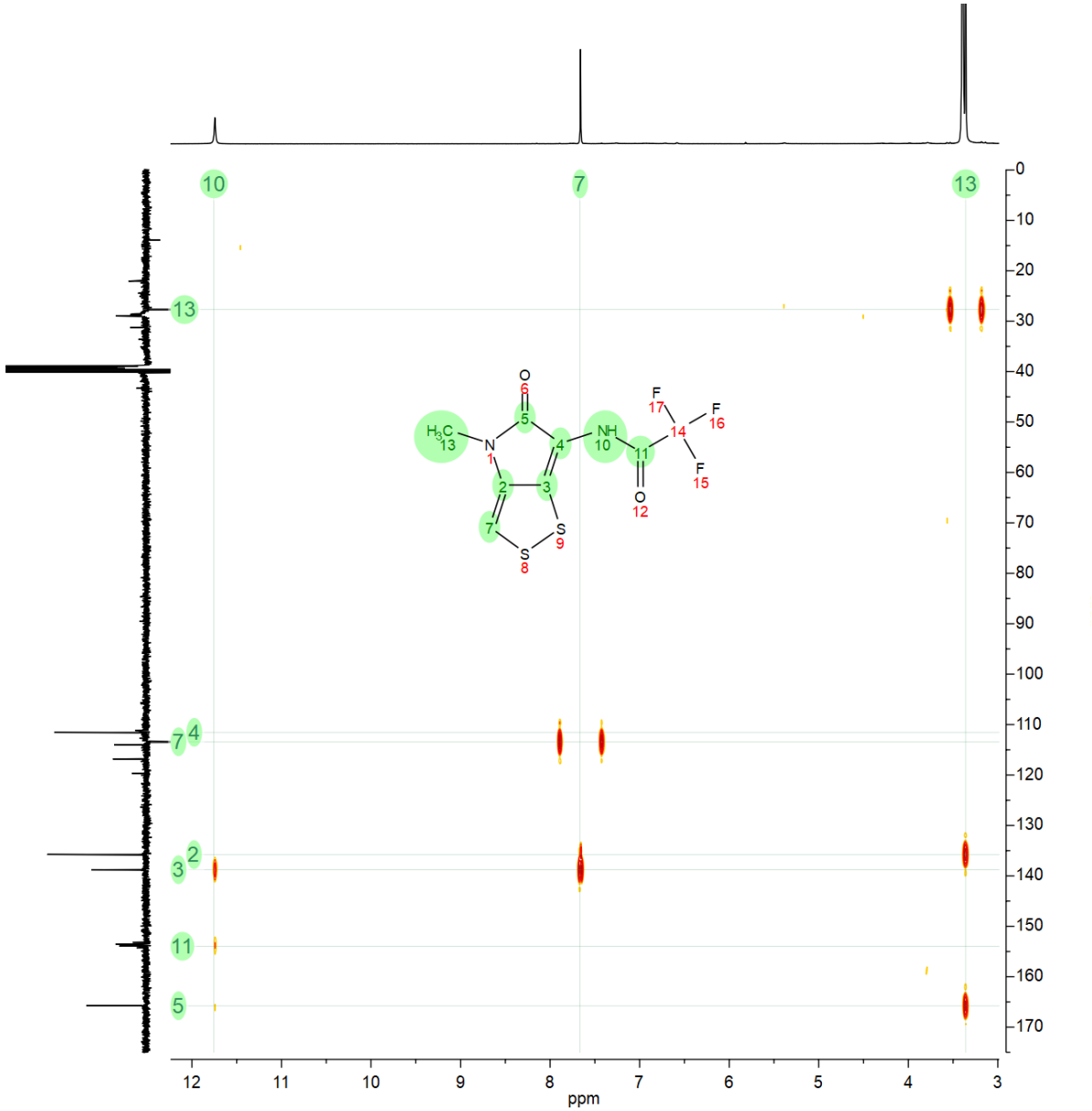

Fig. S41. (^{1}H,^{13}C)-HMBC NMR of CF_3-thiolutin (**9**) (DMSO-d_6, 400 MHz).

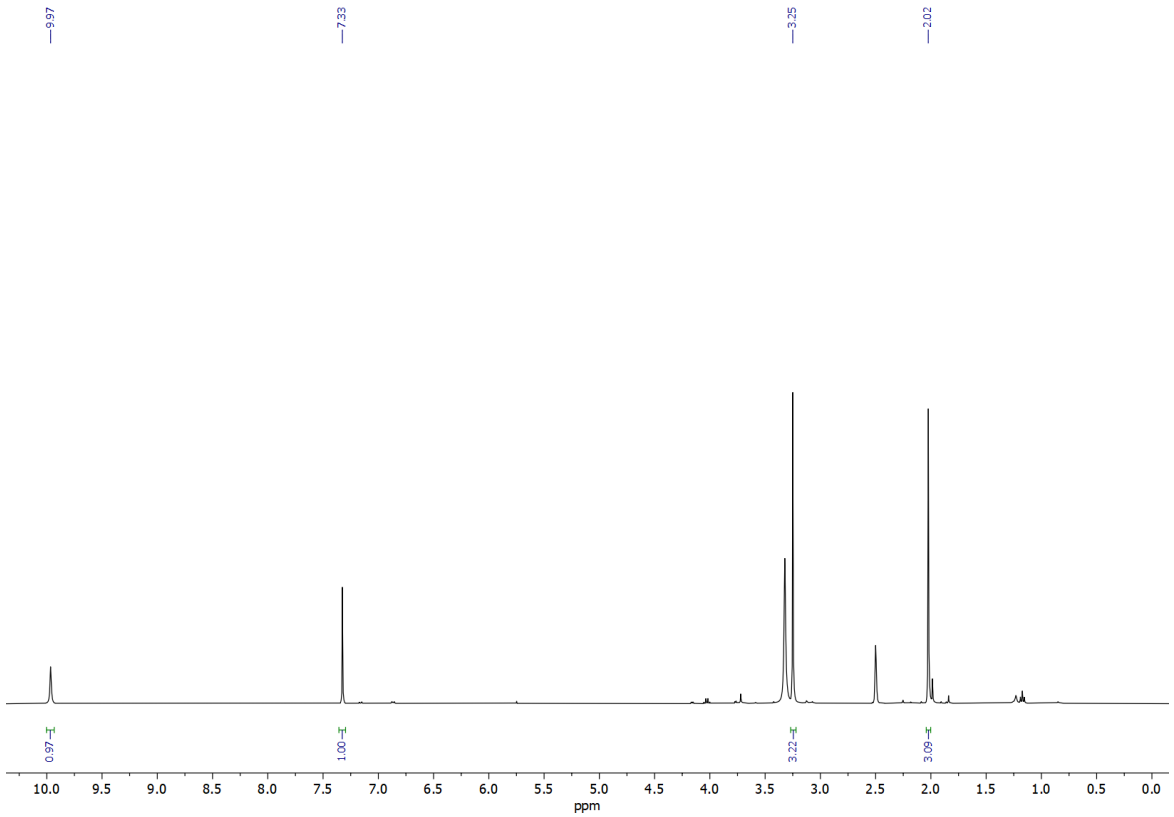

Fig. S42. ^{1}H NMR of thiolutin (**2**) (DMSO-d_6, 400 MHz).

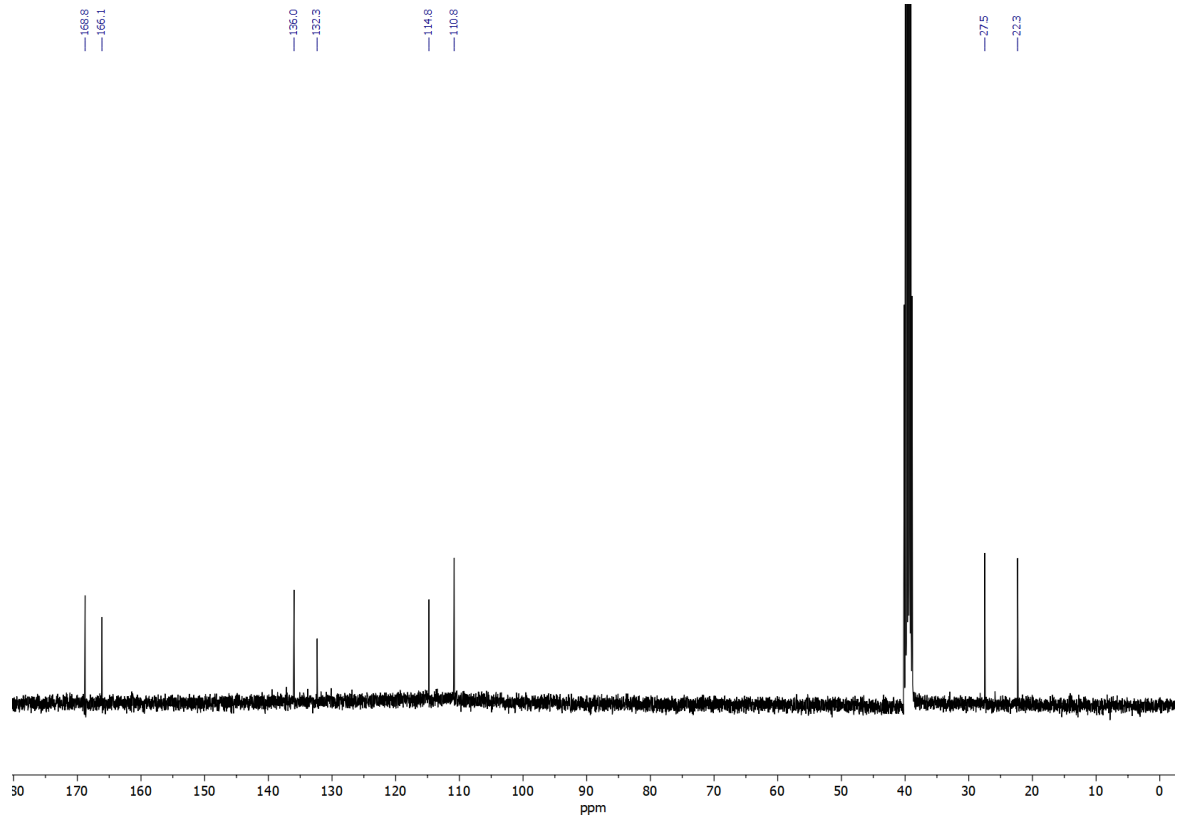

Fig. S43. $^{13}C\{^{1}H\}$ NMR thiolutin (**2**) (DMSO-d_6, 100 MHz).

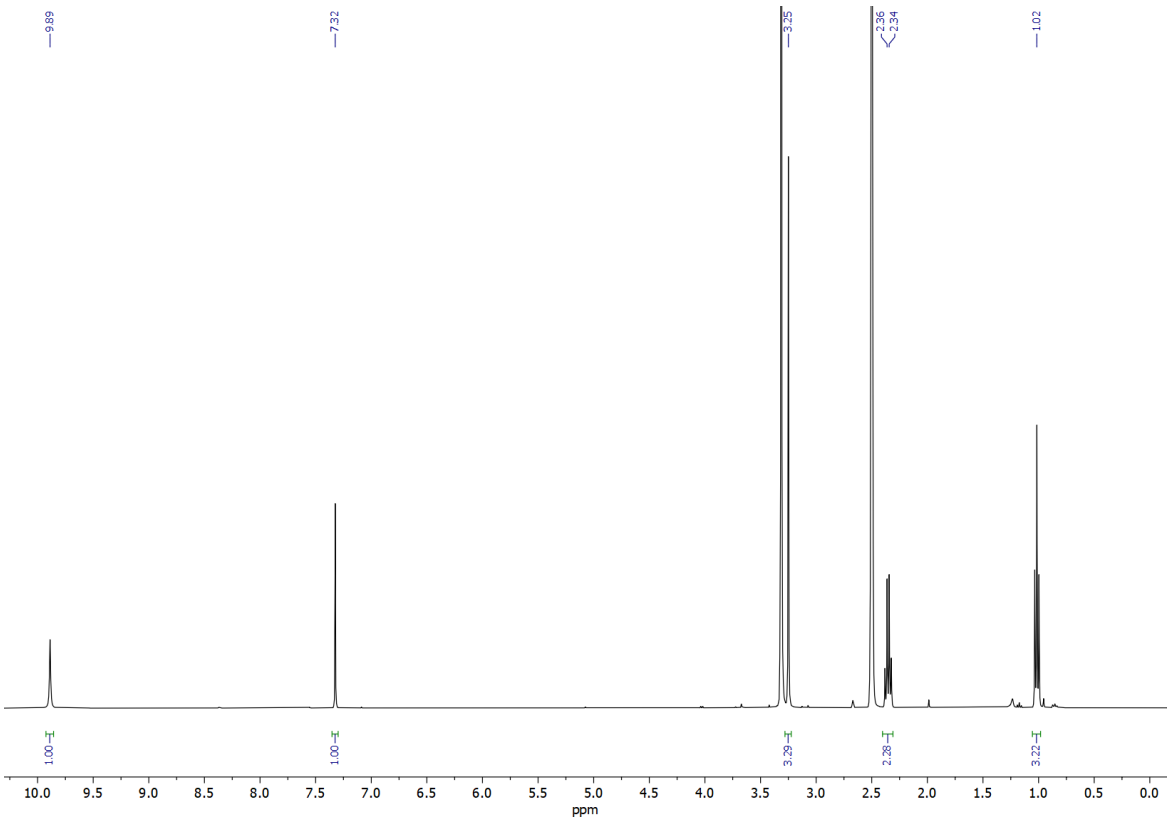

Fig. S44. ^{1}H NMR of aureothricin (**3**) (DMSO-d_6, 400 MHz).

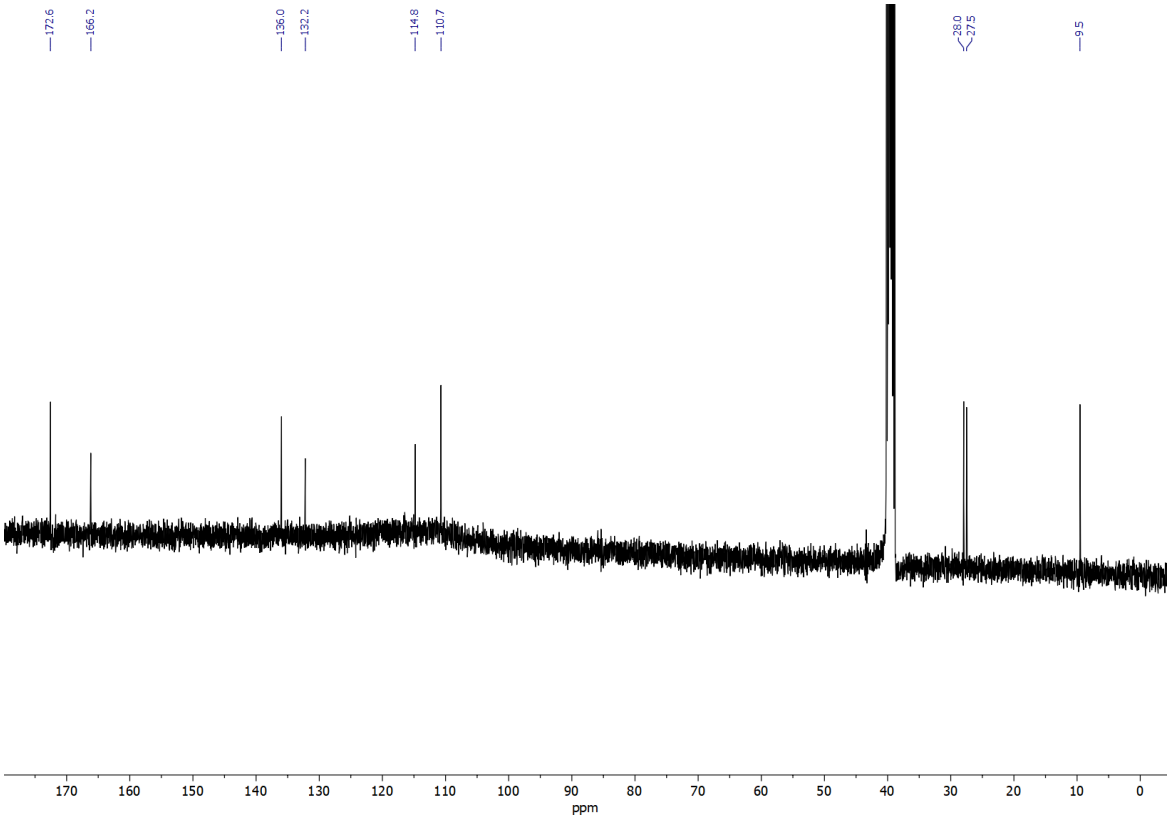

Fig. S45. ^{13}C{^{1}H} NMR of aureothricin (**3**) (DMSO-d_6, 100 MHz).

6) Compound Purities (HPLC Chromatograms)

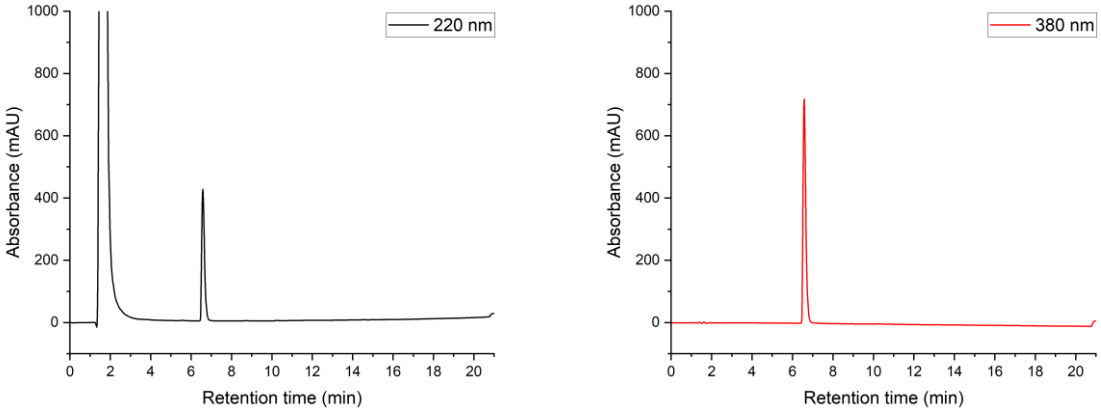

Fig. S46. Analytical HPLC traces of holomycin (**1**); absorbance monitored at 220 nm and 380 nm. The compound was dissolved in MilliQ-H_2O/CH_3CN 1:1, 5% DMF.

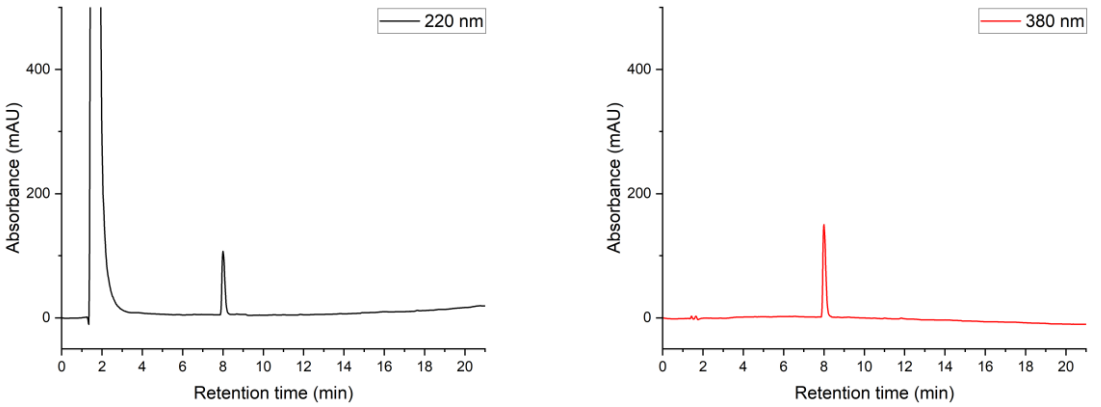

Fig. S47. Analytical HPLC traces of thiolutin (**2**); absorbance monitored at 220 nm and 380 nm. The compound was dissolved in MilliQ-H_2O/CH_3CN 1:1, 5% DMF.

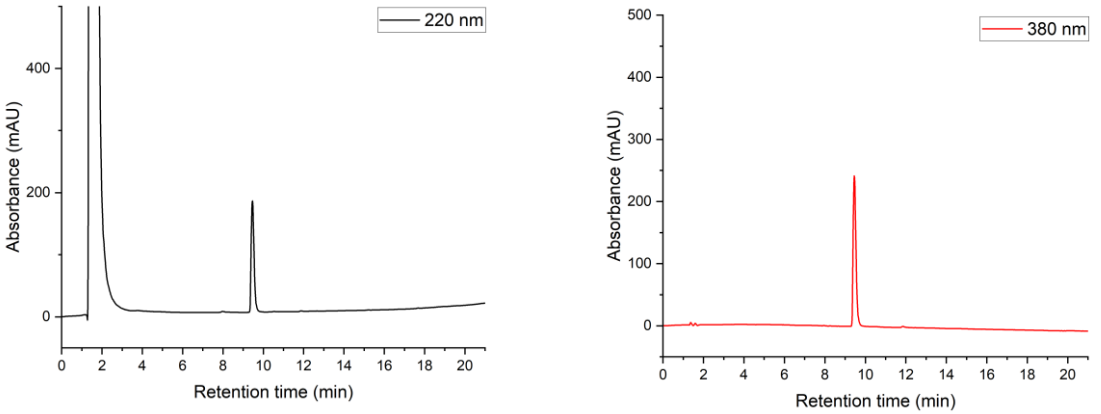

Fig. S48. Analytical HPLC traces of aureothricin (**3**); absorbance monitored at 220 nm and 380 nm. The compound was dissolved in MilliQ-H_2O/CH_3CN 1:1, 5% DMF.